Artesunate - An investigation into polymorphism

S Odendaal

orcid.org/ 0000-0002-0297-9430

Dissertation submitted in fulfilment of the requirements for the degree Masters of Science in Pharmaceutics at the North-West University

Supervisor: Prof W Liebenberg

Co-supervisor: Prof N Stieger

Graduation: May 2020

Student number: 24881953

TABLE OF CONTENTS

Chapter 3

PREPARATION AND CHARACTERISATION METHODS OF ARTESUNATE SOLID-STATE FORMS

Chapter 4

SOLID-STATE FORMS OF ARTESUNATE

Chapter 5

Annexures

ABSTRACT

Artesunate (ART) is a derivative of artemisinin and is used in the treatment of uncomplicated *Plasmodium falciparum* (*P. falciparum*) malaria. Limited and unreliable solid-state and physico-chemical data is currently available for artesunate (ART). Although numerous papers regarding anti-malarial and anti-cancer activities have been published, convincing and consistent information regarding its solid-state forms and physico-chemical properties are lacking.

Polymorphs are different crystal forms of the same compound that have different physical and chemical properties. The most popular definition of polymorphism is 'the ability of *any* compound or molecule to crystallise as more than one crystalline form'.

ART has been reported to occur in different polymorphic forms and there were four entries found in the literature, with reference codes FAHFAV, FAHFAV01, FAHFAV02 and MEXKOP. Three of these entries, FAHFAV, FAHFAV01 and FAHFAV02, are of the same crystalline phase (Form 1) and represent the raw material that is currently commercially found (stereoisomer 10-α-artesunate; orthorhombic with space group $P2_12_12_1$). MEXKOP was found to be the ß-isomer of artesunate.

A novel solvate of artesunate was prepared and identified during this study, i.e. dichloromethane (DCM) solvate, as well as other possibly new polymorphic forms, which still need to be confirmed through further studies. The powder dissolution results of ART were low, due to the poor water solubility of ART. The DCM desolvate, however, surprisingly showed the best powder dissolution results by increasing the dissolution concentration from 23 µg /ml to 38 µg/ml.

To summarise, no new polymorphic forms, nor solvates, nor hydrates, other than Form 1, had been registered in the Cambridge crystallographic data centre (CCDC) for ART to date. Further investigations should be performed to clarify the possibility of the new polymorphic forms, but also to investigate the dissolution results obtained with the DCM desolvate.

Key words: artesunate, polymorphism, solid-state, recrystallisation process, single X-ray diffraction, dichloromethane solvate, physico-chemical properties.

Acknowledgements

I would like to dedicate this masters' dissertation to my grandma, Sophia Van Wyk. She has always been a role model for me and has always motivated me to further my studies, invest in myself and to never have regrets.

I would like to thank my amazing study leader, Prof Wilna Liebenberg, whom without her this dissertation would not have been possible. Thank you for all your patience, expert leadership skills, motivation, excitement and determination throughout this study. I also want to thank Madelein Geldenhuys for her patience, especially for the expert help during lab guidance.

I also want to thank my family for the opportunity to complete my dissertation. Thank you for the support and love throughout this time.

AIM AND OBJECTIVES

Aim:

The aim of this study is to complete a comprehensive solid-state characterisation of artesunate and to identify different polymorphs, solvates and hydrates.

Objectives:

The specific objectives are:

- Standard solid-state form screening;
- Characterisation of all metastable forms identified;
- Dissolution and solubility testing; and
- Accelerated stability testing.

Chapter 1

Overview of different solid-state forms

1.1 Introduction

Solid-state forms of active pharmaceutical ingredients (APIs), such as polymorphs, co-crystals, hydrates, solvates, clathrates and salts, have unique physico-chemical properties that may influence the performance of the pharmaceutical product (Bag & Reddy, 2012). Co-crystals, hydrates, solvates and clathrates are also known as inclusion compounds (Vioglio *et al*., 2017). According to Almarsson and Zaworotko (2004), the key difference between a solvate and a co-crystal is in the 'isolated pure components'. Crystals are referred to as solvates, if one of the components is a liquid at room temperature. If both components are solids at room temperature, the compounds are referred to as co-crystals. Co-crystals are prepared by using a strong hydrogen-bond acceptor and a carboxylic acid, whereas if a proton is transferred from the acid to the base, it becomes a salt (Aakeröy *et al*., 2007).

Polymorphism in molecular compounds is analogous to allotropism in elements. An example of allotropism is demonstrated by carbon that exists as either a cubic diamond, or as hexagonal graphite (Brog *et al*., 2013). Allotropism refers to different forms of an element in which the chemical bonding between the atoms of that same element differs. Polymorphism refers to the different crystal forms belonging to the same, or to a different crystal system (Brog *et al*., 2013).

The exploration of new solid-state forms of existing APIs is important for improving pharmaceutical products. Such investigations can be performed through recrystallisation, co-crystallisation, or salification processes to name a few. These methods modulate the physico-chemical properties of an API, without changing its pharmacological nature (Vioglio *et al*., 2017).

The physical properties of an API are determined by its molecular arrangement. One of the most effective methods for modifying the physical properties of APIs is through salt formation. Many of the pharmaceutical products on the market include actives that are in their salt form. Since this approach requires an API that possesses a suitable ionisable site, basic or acidic, this approach is sometimes very limited (Schultheiss & Newman, 2009).

Chieng *et al*. (2011) states that poor aqueous solubility of an API is a concern in drug development. Amorphous compounds have higher solubility, which leads to better dissolution profiles and better bioavailability. However, amorphous forms do have higher free energy and are therefore more unstable than their crystalline counterparts (Chieng *et al*., 2011).

In most cases, a drug compound is handled in its solid-state form in some stages of the manufacturing process. As a result, the particular solid-state form is of high importance, as it determines the physico-

chemical and handling properties of the bulk powder. Since a change in solid-state form may render a compound toxic or ineffective, quality control must demand the characterisation and elucidation of the solid-state behaviour of all meta-stable forms. The scarcity of marketed pharmaceutical solvates is due to their solid-state meta-stability and the potential toxicity of any included solvents (Douillet *et al*., 2012).

1.2 Importance of the solid-state properties of drug substances

Unexpected polymorphic transformation commonly occurs in pharmaceuticals. Undesirable transformation can happen during processing, or during storage, which may result in product failure. According to Anwar and Zahn (2017), examples of problems that can arise may be a decrease in injection syringeability, suspension caking, and abrasiveness in ointments and in creams. These problems may cause painful application, as well as render them as cosmetically unacceptable. To avoid differences in solubility, dissolution and bioavailability, the most thermodynamically stable polymorph under storage conditions must be chosen.

The chosen solid-state form must preferably have favourable solubility properties and enhance bioavailability. Most often, this is the case with regards to the meta-stable thermodynamic form. The thermodynamic stability of a meta-stable form may unfortunately be compromised by pharmaceutical processes, like tableting, where pressure is applied, or during wet granulation. From a positive point of view, polymorphism can be used to manipulate drugs or compounds and to reveal the advantages of meta-stable compounds, while guaranteeing their stability with respect to solid-state transformation (Anwar & Zahn, 2017).

1.3 Polymorphism

Various definitions for polymorphism exist in the literature (Higashi *et al*., 2016). A popular definition by Haleblian and McCrone (1969) states that: “A polymorph is a solid crystalline phase of a given compound resulting from the possibility of at least two different arrangements of the molecule of the compound in the solid-state. Polymorphism is thus the ability of any molecule or compound to crystallise as more than one distinct crystal species.”

According to Pindelska *et al*. (2017), polymorphism of a substance is the capability to crystallise into two or more crystalline phases, with various arrangements of the components in the crystal lattice. Although polymorphic forms have identical molecular formulae, the systematic arrangement and interaction of the molecules differ.

Polymorphic forms can vary largely with regards to their physico-chemical properties, as well as their solid-state reactivity (Anwar & Zahn, 2017). Bernstein (2002) is of the opinion that inclusion compounds (solvates and co-crystals) and salts are excluded from the definition of polymorphism. Exceptions to this

would be if a salt or inclusion compound exists as different crystal forms, while still possessing identical compositions (Bernstein, 2002). This would be in keeping with the definition of polymorphism by Haleblian and McCrone (1969), in which an inclusion compound and salt would be the “compound”. Nevertheless, the definition of Haleblian and McCrone (1969) remains the most popular definition for polymorphism, i.e. the ability of *any* compound or molecule to crystallise as more than one crystalline form.

1.3.1 Preparation of polymorphs

The literature describes several methods for obtaining unique polymorphic forms. Different polymorphic forms can be prepared through sublimation, crystallisation from a single solvent, evaporation from a binary mixture of solvents, vapour diffusion, thermal treatment and crystallisation from the melt (Guillory, 1999). Different solid-state forms of non-ionisable APIs are generally prepared from solution and from melts, through solid-state transformations, and through the desolvation of solvates, or the dehydration of hydrates.

Recrystallisation is a procedure that can be used by pharmaceutical manufacturers to ensure purity and uniformity of manufactured products, as well as by pharmaceutical researchers, in search for new polymorphs, by altering the recrystallisation conditions. Crystallisation is the creation of a crystalline phase through a process that is initiated by molecular aggregation, which leads to the formation of nuclei and ultimately in crystal growth (Stieger & Liebenberg, 2012).

The most common method for preparing different polymorphic forms is by means of recrystallisation. Crystallisation occurs when super-saturation is achieved. Factors that could influence the crystallisation rate include temperature, the solvent used, the solubility of the solid in the solvent, and the evaporation rate (Kramer & Van Rosmalen, 2000).

According to Rendel *et al*. (2017), nucleation occurs when a new phase is formed, whereas crystal growth takes place when the formed nuclei and crystals continue to grow. Crystal growth, from within a solution involves a solid phase within a liquid phase, which therefore depends upon the interfaces between the two phases, as well as the properties of both. Crystal growth is also regarded as a layer-by-layer development (inter-molecular interaction), where the layers are being characterised by the crystal packing from the cell (Blagden *et al*., 2007).

1.4 Methods employed to obtain distinctive polymorphic forms

In as early as 1897, Ostwald postulated that “A meta-stable polymorph may often be obtained first during the recrystallization from different solvents” (as cited by Gu *et al*., 2001). The less stable form is suspended in a saturated solution, using the solvent-mediated technique. The meta-stable form will

hence dissolve, because its apparent solubility is higher than that of the stable form, resulting in the stable form to crystallise (Figure 1.1) (Gu *et al*., 2001).

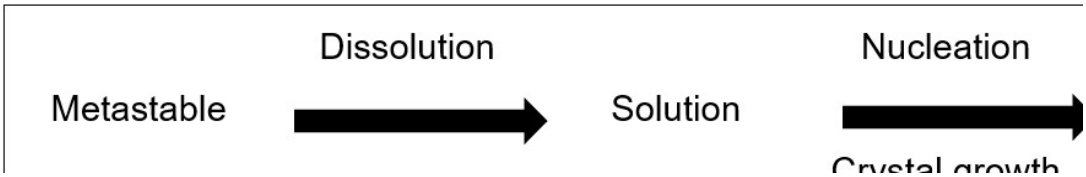

Figure 1.1: Process of solvent-mediated polymorphic transformation (Gu *et al*., 2001).

Lee (2014) lists the following methods through which polymorphs can be prepared and achieved in the pharmaceutical industry.

1. Crystallisation from a blended or single solvent.
2. Crystallisation from structures that are nano-confined.
3. Crystallisation from a melt.
4. Using heat to desolvate a solvate.
5. Using re-slurry to dehydrate a hydrate.
6. Seeding.
7. Solid substrates being thermally activated.
8. Polymorphic transformation.

1.4.1 Types of polymorphs

Due to differences in the thermodynamic properties of polymorphic forms, they can be classified as enantiotropes, or monotropes. The difference between these two thermodynamic terms is 'whether one form can transform reversibly into another below the melting point, or not. In a monotropic system, no reversible transition takes place between the polymorphic forms below the melting point" (Vippagunta *et al*., 2001). Enantiotropic polymorphs can be inter-converted below the melting point of either polymorph, i.e. a reversible transition is possible between polymorphs (Schneer, 1955; Vippagunta *et al*., 2001).

1.5 Inclusion compounds

1.5.1 Solvates

A solvate is the term used where the solvent molecule is part of the crystal structure. Solvates can be incorporated into the crystal lattice in either a stoichiometric, or non-stoichiometric way (Aina, 2012).

Stoichiometric solvates have a fixed ratio of solvent to compound. Non-stoichiometric solvates form where the elemental composition cannot be represented by integers.

The smallest representing molecule in solvates is water (see Hydrates, par.1.5.2).

The terms “solvate” and “solvation” should not be confused. The process by which a solvent molecule surrounds, as well as interacts with each dissolved molecule or ion, is referred to as solvation. Crystallisation in the same space group, with only small distortions of the unit cell dimensions and the same type of molecular network of the host molecule, is referred to as iso-morphic, or iso-structural solvates (Griesser, 2006). Stieger *et al*. (2010) reported rare stoichiometric iso-structural solvates for nevirapine, in which the guest-host ratio varied between 0.5 and 0.32.

According to Shekunov and York (2000), solvates and/or hydrates affect the drug substance and/or drug product through their solubility profiles, as well as their dissolution rates.

Solvates can be identified through thermogravimetric analysis (TGA), during which a prominent weight loss is shown. Weakly bound solvates tend to desolvate before the crystal melts. Strongly bound solvates may even melt right before evaporation. Solvents can either be attached through hydrogen bonding in a discrete site, or can be loosely bound in a relatively open cavity, to form non-stoichiometric solvates (Yu *et al*., 1998).

1.5.2 Hydrates

It is reported that almost one-third of APIs are capable of forming hydrates (Stahl, 1980). During pharmaceutical processing, solids may often encounter water at some stage of manufacturing, e.g. during wet granulation and aqueous film-coating. During storage, the final product and/or the API may also come into contact with water in the atmosphere, or tablets may contain excipients, capable of absorbing moisture, like lactose. Water may also be absorbed onto the surfaces of tablets and bulk powders (Guillory, 1999).

According to Vippagunta *et al*. (2001), crystalline hydrates can be classified into three categories, as summarised in Table 1.1.

Table 1.1: Three classification categories of crystalline hydrates (Vippagunta *et al*., 2001)

Category	Type of hydrate	Example
Class 1	“Isolated site hydrate: Water molecules are isolated from direct contact with each other by intervening drug molecules.	Cephradine dihydrate

Class 2	Channel hydrates: The water molecules included in the lattice lie next to those of adjoining unit cells along an axis of the lattice, forming channels through the crystal. The channel hydrates are sub-classified into two categories:	Ampicillin trihydrate
	1. *Expanded-channel*-, or *non-stoichiometric hydrates*, which may take up additional moisture in the channels when exposed to high humidity, and for which the crystal lattice may expand or contract, as the hydration or dehydration proceeds, effecting changes in the dimensions of unit cells.	Cromolyn sodium
	2. *Planar hydrates*, which are channel hydrates in which water is localised in a two-dimensional order, or plane.	Sodium ibuprofen
Class 3	Ion-associated hydrates, in which the metal ions are co-ordinated with water."	Calteridol calcium

1.5.3 Co-crystals

Co-crystals exist where crystalline solid materials consist of two or more different molecular compounds in a stoichiometric ratio. These components are assembled by non-covalent interactions, like van der Waals interactions and hydrogen bonding, instead of ion pairing (Pindelska *et al*., 2017). Furthermore, two types of co-crystals exist, namely ionic co-crystals (ICCs) and salt co-crystals (SCCs) (Vioglio, 2017). Figure 1.2 demonstrates that SCCs can occur in several molecular arrangements.

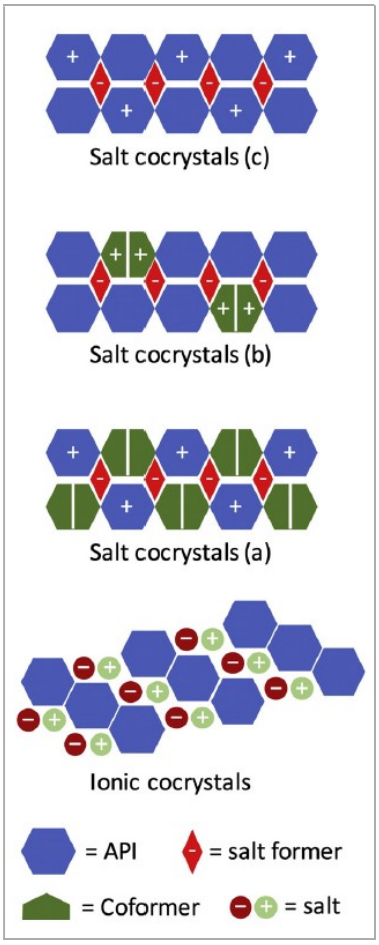

Figure 1.2: Graphic representations of ICCs and SCCs. Depending on the type of SCC, the unit cell is characterised by (a) an API salt and a neutral conformer; (b) a neutral API and a conformer salt; (c) an API salt and a neutral API (Vioglio *et al*., 2017).

1.5.4 Clathrates

Clathrate means 'cage' and is applicable when the solvent is entrapped three-dimensionally within closed voids, also known as cages. The term, clathrate, is used to describe solvates, in which the solvent molecules are entrapped within voids, or cages of the structural lattice of the host molecule, without interacting with them (Griesser, 2006). Clathrates typically represent a crystalline compound in which the structures comprise of a three-dimensional framework of cage-like polyhedrons of one chemical species (Pouchard & Cros, 2014).

1.6 Desolvation and dehydration

During pharmaceutical processing, unstable systems can form due to phase changes that occur during the dehydration and desolvation of pharmaceutical products (Vippagunta *et al*., 2001). Numerous phase

changes can occur, for example after dehydration, when an unstable amorphous phase can be formed. Also, during processing, a thermodynamically unstable form may change into a more stable form, which is less soluble (Morris & Rodriguez-Hornedo, 1993). Normally, mechanical and thermal stress could cause desolvation or dehydration. These transformations affect the stability and physico-chemical properties of the drug compound and will impact the quality of the drug product (Calvo *et al*., 2017).

Perrier and Byrn (1982) found that a few factors of crystal packing exist that may influence, or obstruct the desolvation process, i.e.:

1. The tunnel sizes through which a solvent can escape may differ in size.
2. The compactness of the crystal packing can obstruct a solvent molecule. If the crystals' molecules are packed very closely together, it could be difficult for the molecule to escape.
3. The water chain in a crystal can influence the dehydration process in a few ways, such as:
    a) The extent to which the water chain is in line with the crystal packing.
    b) The relative direction of the water chain in relation to the crystal packing.
    c) The size and form of the water tunnel.
    d) The distances between the contact points of the crystal molecules and the water molecules.
    e) The inter-molecular bonding between the water and crystal molecules, i.e. hydrogen bonding.

1.7 Amorphous forms

Amorphous forms are characterised by the absence of a long-range order of molecular packing (Yu, 2001). According to Thakral *et al*. (2016), an amorphous solid consists of the maximum probable density of defects of numerous dimensionalities, thus the short-range is forced upon its closest neighbour, while the long-range order is misplaced.

Amorphism is induced during pharmaceutical processes, for example during compression and milling (Thakral *et al*., 2016). According to Laitinen *et al*. (2013), amorphous forms can be prepared from a solid into a thermodynamically stable, non-crystalline form (through rapid precipitation from a solution, or rapid cooling from a melt), or from a solid into an amorphous solid (through milling).

The glass transition temperature (T_g) is the temperature where, if a liquid is cooled to below its T_g, a glass form can be obtained (Berthier & Biroli, 2011). The T_g is not a thermodynamic transition, but instead, it is the temperature lower than where the material is too viscous to flow against a rational time. Super-cooling can be used to avoid crystal nucleation, meaning that the melting temperature must be higher than the experimental glass transition temperature (Berthier & Biroli, 2011).

The super-saturation properties of amorphous solids are used to overcome solubility-limited absorption, where the intestinal fluid is already saturated with a drug (Ozaki *et al*., 2012). The apparent solubilities of amorphous forms can be of higher value than their crystalline counterparts, but due to amorphous higher free energy, they are physically unstable and thus transform into the crystalline forms (Thakral *et al*., 2016). The stability of amorphous drugs is attributed to three factors, according to Laitinen *et al*. (2013):

1. The stability against crystallisation is directly related to the miscibility of the drug with a polymer.
2. Compared to the pure amorphous drug, the T_g of the glass solution usually increases due to the polymeric carrier.
3. In solid-solid dispersions, for drug stabilisation, the inter-molecular drug-polymer interactions are of importance.

1.8 Phase transformations in the solid-state

Since any type of transformation in the pharmaceutical industry is most often unplanned, steps should be in place to prevent transformations during manufacturing (Aucamp *et al*., 2015).

According to Vippagunta *et al*. (2001), the following pharmaceutical processes could accelerate phase transitions of compounds during the manufacturing process:

- Drying.
- Lyophilisation.
- Spray drying.
- Grinding.
- Wet granulation.
- Milling (decreases crystallinity, due to the creation of lattice defects, starting at the surface).
- Oven drying.
- Compaction.
- Thermal activation.
- Freeze drying (if water is not removed through this process, the product may be unstable during storage).

Solid-to-solid transformations involve a direct conversion from one solid-state into another, without any occurrence of a solution, or melt phase. Examples include the desolvation, or dehydration of an API, or the polymorphic transformation from one form into another during a process, such as milling (Aucamp *et al*., 2015).

Aucamp *et al*. (2015) proposed the use of 'solvent-interactive transformations' as a collective term for all transformations where solvents are involved. Solvent-interactive transformations are further sub-divided

into three categories, i.e. solution-mediated and solvent-mediated transformations, and solvent catalysed transformation.

Solution-mediated transformation: Occurs when the solid-state is transformed through a solid-solution-solid transformation, where, from the starting material to the final product, no direct transformation is possible, but instead, it is mediated by a solution where the solvent is added to the starting material in a vapour or liquid state. Examples where solution-mediated transformations occurred include:

- During dissolution, where the meta-stable form transformed into the stable form.
- During recrystallisations from solvents to obtain other polymorphic forms and/or solvates and hydrates (Aucamp *et al*., 2015).

Solvent-mediated transformation: A solid-solid transformation, where, from the starting material to the final product, no direct transformation takes place, but instead, it is mediated by a solvent being introduced in the vapour or liquid state, which acts upon an undissolved starting material. Examples included:

- The anhydrous form of an API converted into a hydrate or solvate.
- The crystallisation of an amorphous form into a solvate, or hydrate (Aucamp *et al*., 2015).

Solvent-catalysed transformation: Occurs when a solid-state is transformed through a non-mediated, direct solid-solid transformation, but when a solvent is introduced in the vapour or liquid state, it has a catalytic effect that accelerates the transformation. An example of this type of transformation was when an amorphous form crystallised into an anhydrous form, due to plasticisation (Aucamp *et al*., 2015).

Gas-to-solid vapour deposition is a viable, but low yield option for thermostable APIs that sublimate at a temperature lower than their melting point. It may yield crystalline, or amorphous products. Unless carried out under inert conditions, gas-to-solid transformations may also be acted upon by solvents/moisture (Aucamp *et al*., 2015).

1.9 Conclusion

It is a known fact that pharmaceutical actives have the ability to exist in more than one solid-state form, or that they can form hydrates, or solvates. The exploration of any possible new solid-states of any API is important in improving pharmaceutical products. When determining the stable polymorphic form of an API, manufacturers of pharmaceutical products should be aware of the possible meta-stable forms that may exist and they should take the necessary steps to at least minimise any undesirable transformations (Vioglio *et al*., 2017).

References

Aakeröy, C.B., Fasulo, M.E. & Desper, J. 2007. Cocrystal or salt: does it really matter? *Molecular Pharmaceutics*, 4(3):317-322.

Aina, A.T. 2012. *In situ* monitoring of pharmaceutical crystallisation. Nottingham: University of Nottingham. (Thesis-PhD).

Almarsson, O. & Zaworotko, M.J. 2004. Crystal engineering of the composition of pharmaceutical phases: do pharmaceutical co-crystals represent a new path to improved medicines? *Chemical Communications,* p. 1889-1896.

Anwar, J. & Zahn, D. 2017. Polymorphic phase transitions: macroscopic theory and molecular simulation. *Advanced Drug Delivery Reviews*, 117:47-70.

Aucamp, M.E., Liebenberg, W. & Stieger, N. 2015. Solvent-interactive transformations of pharmaceutical compounds. (*In* Mastai, Y. *ed.* Advanced topics in crystallisation. InTech, DOI: 10.5772/59586. http://www.intechopen.com/books/advanced-topics-in-crystallization/solvent-interactive-transformatios-of-pharmaceutical-compounds). [Date of access: 13 February 2018].

Bag, P.P. & Reddy, C.M. 2012. Screening and selective preparation of polymorphs by fast evaporation method: a case study of aspirin, anthranilic acid, and niflumic acid. *Crystal Growth and Design*, 12(6):2740-2743.

Bernstein, J. 2002. Polymorphism in molecular crystals. Oxford: Clarendon Press. 410p.

Berthier, L. & Biroli, G. 2011. Theoretical perspective on the glass transition and amorphous materials. *Reviews of Modern Physics*, 83(2):587.

Blagden, N., de Matas, M., Gavan, P.T. & York, P. 2007. Crystal engineering of active pharmaceutical ingredients to improve solubility and dissolution rates. *Advanced Drug Delivery Reviews*, 59(7):617-630.

Brog, J.P., Chanez, C.L., Crochet, A. & Fromm, K.M. 2013. Polymorphism, what it is and how to identify it: a systematic review. *RSC Advances*, 3(38):16905-16931.

Calvo, N.L., Maggio, R.M. & Kaufman, T.S. 2017. Chemometrics-assisted solid-state characterization of pharmaceutically relevant materials: polymorphic substances. *Journal of Pharmaceutical and Biomedical Analysis,* 147:518-537.

Chieng, N., Rades, T. & Aaltonen, J. 2011. An overview of recent studies on the analysis of pharmaceutical polymorphs. *Journal of Pharmaceutical and Biomedical Analysis,* 55(4):618-644.

Douillet, J., Stevenson, N., Lee, M., Mallet, F., Ward, R., Aspin, P., Dennehy, D.R. & Camus, L. 2012. Development of a solvate as an active pharmaceutical ingredient: developability, crystallisation and isolation challenges. *Journal of Crystal Growth*, 342(1):2-8.

Griesser, U.J. 2006. The importance of solvates, edited by Hilfiker, R. Weinheim: Wiley-VCH. https://onlinelibrary.wiley.com/doi/10.1002/3527607889.ch8. [Date of access: 01 August 2019].

Gu, C.H., Young, V. & Grant, D.J. 2001. Polymorph screening: influence of solvents on the rate of solvent-mediated polymorphic transformation. *Journal of Pharmaceutical Sciences*, 90(11):1878-1890.

Guillory, J.K. 1999. Generation of polymorphs, hydrates, solvates and amorphous solids. (*In* Brittain, H.H. *ed.* Polymorphism in pharmaceutical solids. New York: Marcel Dekker. p. 183-226).

Haleblian, J. & McCrone, W. 1969. Pharmaceutical applications of polymorphism. *Journal of Pharmaceutical Sciences*, 58(8):911-929.

Higashi, K., Ueda, K. & Moribe, K. 2016. Recent progress of structural study of polymorphic pharmaceutical drugs. *Advanced Drug Delivery Reviews*, 117:71-85.

Kramer, H.J.M. & Van Rosmalen, G.M. 2000. Crystallization. *Encyclopedia of separation science*, p64-84. https://www.sciencedirect.com/science/article/pii/B0122267702000314 [Date of access: 23 March 2019].

Laitinen, R., Löbmann, K., Strachan, C.J., Grohganz, H. & Rades, T. 2013. Emerging trends in the stabilization of amorphous drugs. *International Journal of Pharmaceutics*, 453(1):65-79.

Lee, E.H. 2014. A practical guide to pharmaceutical polymorph screening and selection. *Asian Journal of Pharmaceutical Sciences*, 9(4):163-175.

Morris, K.R. & Rodriguez-Hornedo, N. 1993. Hydrates. (*In* Swarbick, J., Boylan, J.C. *eds*. Encyclopedia of pharmaceutical technology, vol 7. New York: Marcel Dekker. p. 393-441).

Ozaki, S., Kushida, I., Yamashita, T., Hasebe, T., Shirai, O. & Kano, K. 2012. Evaluation of drug supersaturation by thermodynamic and kinetic approaches for the prediction of oral absorbability in amorphous pharmaceuticals. *Journal of Pharmaceutical Sciences*, 101(11):4220-4230.

Pindelska, E., Sokal, A. & Kolodziejski, W. 2017. Pharmaceutical cocrystals, salts and polymorphs: advanced characterization techniques. *Advanced Drug Delivery Reviews*, 117:111-146.

Perrier, P. & Byrn, S.R. 1982. Influence of crystal packing on the solid-state desolvation of purine and pyrimidine hydrates: loss of water of crystallization from thymine monohydrate, cytosine monohydrate, 5-nitrouracil monohydrate, and 2'-deoxyadenosine monohydrate. *The Journal of Organic Chemistry*, 47(24):4671-4676.

Pouchard, M. & Cros, C. 2014. The early development of inorganic clathrates. (*In* Nolas, G.S. *ed.* The physics and chemistry of inorganic clathrates. Dordrecht: Springer. p. 1-33).

Rendel, P.M., Gavrieli, I., Wolff-Boenisch, D. & Ganor, J. 2017. Towards establishing a combined rate law of nucleation and crystal growth: the case study of gypsum precipitation. *Journal of Crystal Growth*, 485:28-40.

Schneer, C.J. 1955. Polymorphism in one dimension. *Acta Crystallographica*, 8(5):279-285.

Schultheiss, N. & Newman, A. 2009. Pharmaceutical co-crystals and their physico-chemical properties. *Crystal Growth and Design*, 9(6):2950-2967.

Shekunov, B.Y. & York, P. 2000. Crystallization processes in pharmaceutical technology and drug delivery design. *Journal of Crystal Growth*, 211(1-4):122-136.

Stahl, H.P. 1980. The problems of drug interactions with excipients. (*In* Braimar, D.D. *ed.* Towards better safety of drugs and pharmaceutical products. North-Holland: Elsevier. Biomedical press. 265-280p).

Stieger, N., Liebenberg, W., Wessels, J.C., Samsodien, H. & Caira, M.R. 2010. Channel inclusion of primary alcohols in isostructural solvates of the antiretroviral nevirapine: an X-ray and thermal analysis study. *Structural Chemistry*, 21:771-777.

Stieger, N. & Liebenberg, W. 2012. Recrystallization of active pharmaceutical ingredients. (*In* Andreeta, M.R.B. *ed*. Crystallization / Book 1. ISBN 979-953-307-624-8).

Thakral, S., Terban, M.W., Thakral, N.K. & Suryanarayanan, R. 2016. Recent advances in the characterization of amorphous pharmaceuticals by X-ray diffractometry. *Advanced Drug Delivery Reviews*, 100:183-193.

Vioglio, P.C., Chierotti, M.R. & Gobetto, R. 2017. Pharmaceutical aspects of salt and cocrystal forms of APIs and characterization challenges. *Advanced Drug Delivery Reviews*, 117:86-110.

Vippagunta, S.R., Brittain, H.G. & Grant, D.J.W. 2001. Crystalline solids. *Advanced Drug Delivery Reviews*, 48:3-26.

Yu, L. 2001. Amorphous pharmaceutical solids: preparation, characterization and stabilization. *Advanced Drug Delivery Reviews*, 48(1):27-42.

Yu, L., Reutzel, S.M. & Stephenson, G.A. 1998. Physical characterization of polymorphic drugs: an integrated characterization strategy. *Pharmaceutical Science and Technology Today*, 1(3):118-127.

Chapter 2

Artesunate literature study

2.1 Introduction

Artesunate (ART) is a derivative of artemisinin. To date, not much valid information about its physico-chemical properties and solid-state forms is available in the literature. Artemisinin-based combination therapies are used in the treatment of uncomplicated *Plasmodium falciparum* (*P. falciparum*) malaria (Zwang *et al*., 2009). This specific type of malaria is currently being reduced by using combination therapies of different types of artemisinin derivatives, especially in combination with ART (Badshah *et al*., 2018; Zwang *et al.,* 2009).

2.2 Physico-chemical properties

ART is an almost white, fine, crystalline powder that is odourless. The melting point of ART is between 131ºC and 135ºC and it would ignite spontaneously at temperatures above 200ºC (USP, 2012). The pH of ART is between 3.5 and 4.5 and it is freely soluble in acetone and ethanol (USP, 2012). According to the USP (2012), ART is water soluble, while Tran *et al.* (2015) report that it has poor aqueous solubility and that it is easily degraded in acidic conditions.

2.3 Structural formula and chemical name

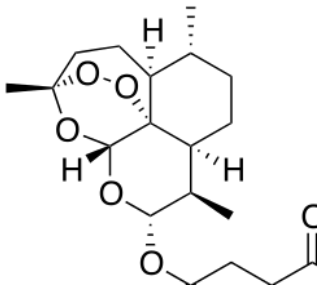

Figure 2.1: Molecular structure of artesunate (ART) (Wikimedia commons, 2018).

The chemical name of ART is mono-[(3R,5aS,6R,8aS,9R,10R,12R,12aR)-decahydro-3,6,9-trimethyl-3,12-epoxy-12H-pyrano[4,3-j]-1,2-benzodioxepin-10-yl] ester and it is also known as artesunic acid, or butanedioic acid (International Pharmacopoeia, 2017).

2.4 Molecular formula and weight

The molecular formula of ART is $C_{19}H_{28}O_8$ and its molecular weight equals 384.425 g/mol (National centre for biotechnology information, 2018).

2.5 Solid-state forms

Some polymorphic forms of ART are described in the Cambridge crystallographic data centre (CCDC) (as cited by Caira, 2019). Four entries, with reference codes FAHFAV, FAHFAV01, FAHFAV02 and MEXKOP, are reported. The three polymorphs, FAHFAV, FAHFAV01, FAHFAV02 (Form 1) are of the same crystalline phase and represent the raw material that is currently commercially available (stereoisomer 10-α-ART; orthorhombic with space group $P2_12_12_1$) (as cited by Caira, 2019).

Lisgarten *et al*. (2002) also report that the crystals, recrystallised from methanol, are orthorhombic, with space group $P2_12_12_1$. They hence also represent the already published Form 1. MEXKOP was found to be the ß-isomer of ART (as cited by Caira, 2019).

To summarise, no other polymorphic forms of ART, nor solvates, nor hydrates, other than those of Form 1, are currently registered in the CCDC.

2.6 Pharmacology

2.6.1 Indication

According to Zwang *et al.* (2009), the artemisinin-ART combination is used in the treatment of uncomplicated *P. falciparum* malaria. Haynes *et al.* (2007) report that ART is unsuited when used in combination with basic quinolines. Artemisinin-derivative combinations reduce gametocyte carriage and infectivity, because they are fast acting and effective anti-malarials (Osorio *et al.,* 2007). In addition, ART is also used in the treatment of human melanomas and as chemotherapy for the majority of cancers (Xu *et al.,* 2019*).*

2.6.2 Mechanism of action

The reduction of artemisinin, a sesquiterpene lactone endoperoxide, leads to ART, which is a hemisuccinate derivative of dihydroartemisinin (WHO, 2015). Its mechanism of action is not well defined in the literature, but according to the World Health Organization (WHO) (2015), it involves a loss of the endoperoxide bridge and a ’cation-mediated generation of reactive intermediates’.

2.6.3 Resistance

ART in combination with sulfadoxine-pyrimethamine has become more resistant to *Plasmodium vivax* malaria than *P. falciparum*, and it therefore compromises the effectiveness of the ART combination (WHO, 2015). Although ART in combination therapy is dependent on the *P. falciparum* resistance against the artemisinin-combination, the use of ART monotherapies have increased, without adversely affecting patient tolerability (Anon, 2004).

2.7 Pharmacokinetics

2.7.1 Absorption and distribution

When ART is prepared as a solution in the presence of amodiaquine, it is quickly hydrolysed *in-vivo* to dihydro-artemisinin, which is the main metabolite that gives the anti-malarial effect (Kauss *et al.,* 2010). The distribution of ART is body weight dependent, meaning that if a child is given ART intravenously (IV), it would require a somewhat higher dosage, because of the larger apparent volume (WHO, 2015).

2.7.2 Metabolism and excretion

Since ART is classified in the Biopharmaceutical classification system (BCS) as a Class II drug, it has good permeability, but low solubility (Setyawan *et al.,* 2015). ART disintegrates under aqueous acidic conditions and delivers a considerable amount of peroxyhemiacetal, which disintegrates (under basic or acidic conditions) into 2-deoxyartemisinin (Haynes *et al*., 2007).

The WHO (2015) guidelines for the treatment of malaria recommend ART in combination with a partner drug. ART is an artemisinin derivative and is very fast acting (half-life of 26 min), while the partner drug is longer acting and slowly eliminated (Kauss *et al.,* 2010). Dihydro-artemisinin is roughly 93% plasma protein bound and it is metabolised in the gut and liver by glucuronidation, after which it is excreted in the urine (WHO, 2015).

2.7.3 Dosage and administration

Since ART is used to treat severe malaria, it can be administered intravenously, or intramuscularly for about 24 hours. Larger children and adults receive 2.4 mg/kg for one day. A child who weighs less than 20 kg needs a slightly higher dosage, i.e. 3 mg/kg for one day, to ensure equal drug distribution. Once a patient has stabilised after 24h of the initial ART treatment, oral therapy can proceed for 3 days with an ART combination product (WHO, 2015).

2.8 Side-effects, precautions, interactions and contra-indications

2.8.1 Side-effects and precautions

Precautions: Limited human data is available regarding the use of ART monotherapy in the first trimester of pregnancy, whereas ART and quinine can be used in combination in the first trimester without hesitation, until other medication is available (Rossiter *et al*., 2014).

Adverse effects: See Table 2.1 below.

Table 2.1: Adverse effects of ART monotherapy (Rossiter *et al*., 2014)

Common	Rare
• Dizziness • Nausea • Anorexia • Vomiting	• Animal studies showed neurotoxicity, no evidence in humans • Anemia • Neutropenia • Reticulocyte count reduced • Eosinophilia

2.8.2 Interactions and contra-indications

The human immunodeficiency virus (HIV) has been linked to malaria, because an increasing number of malaria related passings and severe malaria have been observed in HIV patients (WHO, 2015). According to a study by German *et al.* (2007), the risk for neutropenia had increased after 14 days of treatment, while hepatotoxicity was also reported where ART had been used in combination with amodiaquine and efavirenz (German *et al.,* 2007). With nevirapine, there was an increase in plasma concentration when used in combination with ART (WHO, 2015).

2.9 Registered pharmaceutical preparations containing artesunate

Some of the currently registered ART preparations available in the retail market and in hospitals include Artiquin, Araqal, Artiwel and Artesa (Anon, 2019).

2.10 Conclusion

Since artesunate is classified as a Class II drug by the Biopharmaceutical classification system, it makes sense to explore the possibility of more solid-state forms of ART, aimed at improving its solubility. Such investigations would furthermore unveil the possibility as to whether ART would produce polymorphic forms, other than those already reported in the available literature, when prepared from different solvents.

References

Anon. 2004. International artemisinin study group: artesunate combinations for treatment of malaria: meta-analysis. *The Lancet*, 363:9-17.

Anon. 2019. Artesunate brands in Pakistan. http://www.druginfosys.com/availablebrands.aspx?query=50%20mg&form=Tabs&drugCode=2188&drugName=Artesunate&Ing==1. [Date of access: 16 April 2019].

Badshah, S.L., Ullah, A., Ahmad, N., Almarhoon, Z.M. & Mabkhot, Y. 2018. Increasing the strength and production of artemisinin and its derivatives. *Molecules*, 23(1):100.

Caira, M.R. 2019. Artesunate polymorphic forms. Technical report.

German, P., Greenhouse, B., Coates, C., Dorsey, G., Rosenthal, P.J., Charlebois, E., Lindegardh, N., Havlir, D. & Aweeka, F.T. 2007. Hepatotoxicity due to a drug interaction between amodiaquine plus artesunate and efavirenz. *Clinical Infectious Diseases*, 44(6):889-891.

Haynes, R.K., Chan, H.W., Lung, C.M., Ng, N.C., Wong, H.N., Shek, L.Y., Williams, I.D., Cartwright, A. & Gomes, M.F. 2007. Artesunate and dihydroartemisinin (DHA): unusual decomposition products formed under mild conditions and comments on the fitness of DHA as an antimalarial drug. *ChemMedChem: Chemistry Enabling Drug Discovery*, *2*(10):1448-1463.

International Pharmacopoeia. 2017. 7th *ed*. http://apps.who.int/phint/pdf/b/Jb.6.1.34.pdf. [Date of access: 17 July 2018].

Kauss, T., Fawaz, F., Guyot, M., Lagueny, A.M., Dos Santos, I., Bonini, F., Olliaro, P., Caminiti, A. & Millet, P. 2010. Fixed artesunate-amodiaquine combined pre-formulation study for the treatment of malaria. *International Journal of Pharmaceutics*, 395(1-2):198-204.

Lisgarten, J.N., Potter, B., Palmer, R.A., Chimanuka, B. & Aymami, J. 2002. Structure, absolute configuration, and conformation of the antimalarial drug artesunate. *Journal of Chemical Crystallography*, 32:43-48.

National centre for biotechnology information. 2018. PubChem compound database; CID=65664. https://pubchem.ncbi.nlm.nih.gov/compound/Artesunate#section=Top. [Date of access: 17 July 2018].

Osorio, L., Gonzalez, I., Olliaro, P. & Taylor, W.R. 2007. Artemisinin-based combination therapy for uncomplicated *Plasmodium falciparum* malaria in Colombia. *Malaria Journal*, 6(1):25.

Ph. Int. *see* International Pharmacopoeia.

Rossiter, D., Blockman, M. & Barnes, K.I., *eds.* 2014. South African medicine formulary (SAMF). 11th ed. South Africa: Health and Medical Publishing Group. 516-520p.

Setyawan, D., Wardhana, N.K. & Sari, R. 2015. Solubility, dissolution test and antimalarial activity of artesunate nicotinamide co-crystal prepared by solvent evaporation and slurry methods. *Asian Journal of Pharmaceutical and Clinical Research*, 8(2):164-166.

Tran, T.H., Nguyen, T.D., Poudel, B.K., Nguyen, H.T., Kim, J.O., Yong, C.S. & Nguyen, C.N. 2015. Development and evaluation of artesunate-loaded chitosan-coated lipid nanocapsule as a potential drug delivery system against breast cancer. *AAPS PharmSciTech,* 16(6):1307-1316.

United States Pharmacopeia. 2012. Safety data sheet. http://chem.pharmacy.psu.ac.th/chemical/msds/artesunate.pdf. Artesunate. Version #2. [Date of access: 21 May 2018].

USP *see* United States Pharmacopeia.

WHO *see* World Health Organization.

Wikimedia commons. 2018. Artesunate. https://commons.wikimedia.org/wiki/Category:Artesunate. [Date of access: 16 April 2018].

World Health Organization (WHO). 2015. Guidelines for the treatment of malaria. World Health Organization. https://www.who.int/malaria/publications/atoz/9789241549127/en8/ [Date of access: 16 April 2019].

Xu, R., Han, T., Shen, L., Zhao, J. & Lu, X.A. 2019. Solubility determination and modelling for artesunate in binary solvent mixtures of methanol, ethanol, isopropanol, and propylene glycol water. *Journal of Chemical and Engineering Data,* 64(2):755-762.

Zwang, J., Olliaro, P., Barennes, H., Bonnet, M., Brasseur, P., Bukirwa, H., Cohuet, S., D'Alessandro, U., Djimdé, A., Karema, C. & Guthmann, J.P. 2009. Efficacy of artesunate-amodiaquine for treating uncomplicated *falciparum* malaria in sub-Saharan Africa: a multi-centre analysis. *Malaria Journal*, 8(1):203.

Chapter 3

Preparation and characterisation methods of artesunate solid-state forms

3.1 Introduction

During this polymorphic study of artesunate (ART), various characterisation techniques were employed to gather the necessary information for identifying any possible new solid-state forms of this active pharmaceutical ingredient (APIs). All of the standard solid-state characterisation techniques, like X-ray powder diffractometry, infrared spectroscopy and thermal analysis, were used to characterise the recrystallisation products that had been prepared in this study.

3.2 Preparation of artesunate (ART) solid-state forms

3.2.1 Recrystallisation method

Approximately 1 g of ART powder was added to glass beakers of various sizes, depending on the required volumes of the different solvents used to prepare the super-saturated solutions. The glass beakers, containing the prepared solutions, were then sealed with a layer of parafilm® and left undisturbed for a reasonable period of time in a closed cabinet, to allow for the evaporation of the solvents at room temperature. All crystal forms of ART were obtained by using the slow recrystallisation method. Table 3.1 summarises all the solvents and water dilutions used to yield the different recrystallisation products.

Table 3.1: Solvents used for the recrystallisation of artesunate

Recrystallisation solvents used (acronym used in brackets)	**Water dilutions**
Acetone (**@**)	-
Acetonitrile (**AcN**)	-
1-Butanol (**B1**)	-
2-Butanol (**B2**)	-
Chloroform (**Cf**)	-
Dichloromethane (**DCM**)	-
Diethylether (**DiE**)	-

Ethanol (**Et**)	➢ Ethanol (90%) & Water (10%) ➢ Ethanol (80%) & Water (20%) ➢ Ethanol (70%) & Water (30%) ➢ Ethanol (60%) & Water (40%) ➢ Ethanol (50%) & Water (50%) ➢ Ethanol (40%) & Water (60%)
Ethyl acetate (**EtAt**)	-
Methanol (**Mt**)	➢ Methanol (90%) & Water (10%) ➢ Methanol (70%) & Water (30%) ➢ Methanol (50%) & Water (50%)
1-Propanol (**P1**)	➢ 1-Propanol (90%) & Water (10%) ➢ 1-Propanol (70%) & Water (30%) ➢ 1-Propanol (50%) & Water (50%)
2-Propanol (**P2**)	-
Tetrahydrofuran (**THF**)	-

3.3 Methods of characterisation

3.3.1 X-ray crystallography

3.3.1.1 X-ray powder diffractometry (XRPD)

X-ray powder diffraction patterns were obtained using a PANalytical Empyrean diffractometer (PANalytical, Almelo, Netherlands). The measurement conditions were: target, Cu; voltage, 40 kV; current, 30 mA; divergence slit, 2 mm; anti-scatter slit, 0.6 mm; detector slit, 0.2 mm; monochromator; scanning speed, 2°/min (step size, 0.025°; step time, 1.0 sec).

3.3.1.2 Single X-ray crystallography (SXRD)

Single crystals of good quality were subjected to SXRD determinations. The technical detail for the measurement of the dichloromethane solvate crystal were as follows: A total of 5 500 frames were collected. The total exposure time was 3.06 hours. The frames were integrated with the Bruker SAINT (Bruker, Billerica, USA) software package, using a narrow-frame algorithm. The integration of the data, using a hexagonal unit cell, yielded a total of 109 687 reflections to a maximum θ angle of 28.37° (0.75 Å resolution). The final cell constants of a = 10.5907(12) Å, c = 37.045(4) Å, volume = 3598.4(13) $Å^3$, were based upon the refinement of the XYZ-centroids of 9 918 reflections above 20 σ(I) with 4.441°<2θ<

52.55°. Data was corrected for absorption effects, using the multi-scan method (SADABS). The ratio of minimum to maximum apparent transmission was 0.916.

3.3.2 Simultaneous thermal analysis (STA)

STA simultaneously measures the mass loss (thermogravimetric analysis (TGA)) and heat flow (differential scanning calorimetry (DSC)) of a sample during the heating process. With this combined technique, information about the mass loss, melting point, glass transition, solid-state transformation(s), loss of solvent(s) and the degradation of a sample can be obtained (Brown, 2001). A Mettler DTG 3^{+} (Mettler Toledo, Greifensee, Switzerland) simultaneous thermal analysis instrument was used to record the DSC and TGA thermograms. Powder test samples, weighing approximately 3 - 8 mg each, were placed in individual open aluminum cells (100 µl) and heated to an end temperature of 200°C at a heating rate of 10°C/min, with a nitrogen gas flow of 35 ml/min.

3.3.3 Microscopy

3.3.3.1 Hot-stage microscopy (HSM)

The hot-stage microscope that was used in this study was a Nikon Eclipse 50i microscope (Tokyo, Japan), linked with a programmable Linkam heating stage (Surry, UK) and a Nikon DS-Fi1 camera (Tokyo, Japan). The imaging software that was used to capture the photomicrographs was the NIS Elements, F package, version 3.22. The heating rate of the hot-stage was set to correlate with the heating rate used in the STA experiment.

3.3.3.2 Stereo microscopy

The stereo microscopy system uses only one powerful cold light LED, which provides an ideal digital, ripple-free illumination imaging (Anon., 2019). A Leica KL 200 LED microscope (Leica Microsystems, Heerbrugg, Switserland), linked to the Motic Images Advanced 3.2 software, was used to capture photomicrographs of the recrystallised crystals.

3.3.3.3 Scanning electron microscopy (SEM)

An FEI Quanta 200 FEG SEM, with an X-Max 20 EDS system (FEI, USA), were used to obtain micrographs of the various crystal and amorphous forms. In preparation, samples were adhered to a small piece of carbon tape, mounted onto a metal stub and coated with a gold-palladium film (Eiko Engineering ion Coater IB-2, USA).

3.3.4 Fourier-transform infrared spectroscopy (FT-IR)

Fourier-transform infrared spectroscopy (FT-IR) is a technique that is used to obtain information regarding the structure and molecular conformation of a sample, by measuring the vibration modes of the bonded atoms (Bernstein, 2002; Rodriguez-Spong *et al*., 2004).

IR-spectra were recorded on a Bruker Alpha Platinum spectrometer (Bruker, Billerica, USA) over a range of 400 - 4000 cm^{-1}. The Alpha Platinum Module has the ATR accessory, designed for minimal operator induced variations, by offering preparation free sampling and excellent reproducibility. The OPUS software was used to analyse the data.

3.3.5 Powder dissolution studies

A VanKel700 (Varian, Palo Alto, USA) dissolution bath was used for the dissolution testing. USP apparatus 2 (paddle) was set up at 37°C at a rotational speed of 75 rpm, and 900 mL distilled water as dissolution medium was added to each of the six dissolution vessels. Approximately 50 mg each of powder samples was weighed into 10 mL test tubes, to which 25 mg glass beads (≤ 106 µm) (Sigma-Aldrich, South Africa) were added. 5 mL of dissolution medium, maintained at 37°C, was added to each test tube. The mixtures were agitated for a period of 120 seconds, using a vortex mixer. The resulting mixtures was each transferred into a dissolution vessel. 3 mL of solution was withdrawn from each dissolution vessel at predetermined time intervals (see Table 3.2). The dissolution medium was not replaced after sampling, since a super-saturated solution was required to observe solution mediated transformations. After withdrawal, the samples were each filtered through a 0.45 µm PVDF filter into a high performance liquid chromatography (HPLC) vial. The filtered solutions were analysed by HPLC. A typical powder dissolution time schedule that was used for sampling during the dissolutions tests is demonstrated in Table 3.2.

Table 3.2: Powder dissolution sampling time schedule used

Powder dissolution: Artesunate raw material								
Vessel	**Vortex time intervals**	**5 min**	**10 min**	**20 min**	**30 min**	**60 min**	**120 min**	**180 min**
1	0 min	5 min	10 min	20 min	30 min	60 min	2h00	3h00
2	2 min	7 min	12 min	22 min	32 min	1h02	2h02	3h02
3	4 min	9 min	14 min	24 min	34 min	1h04	2h04	3h04
4	6 min	11 min	16 min	26 min	36 min	1h06	2h06	3h06
5	8 min	13 min	18 min	28 min	38 min	1h08	2h08	3h08
6	10 min	15 min	20 min	30 min	40 min	1h10	2h10	3h10

3.3.6 High performance liquid chromatography (HPLC)

For the HPLC analysis of ART, a Shimadzu chromatographic system (Shimadzu, Kyoto, Japan) was used. A Phenomenex® Luna C18 (5 µm), 150 mm x 4.6 mm reverse phase column was used as stationary phase. A mobile phase, consisting of 44 parts of acetonitrile and 56 parts of 0.01 M phosphate buffer at pH 3.0 (pH adjusted with phosphoric acid), was used at a flow rate of 1.0 mL/min. All samples were analysed at a wavelength of 216 nm. The column temperature was maintained at 30°C. The injection volume for each sample was 20 µl (International Pharmacopoeia, 2017). The method used had been validated, with a linear regression of R^2 = 0.9993.

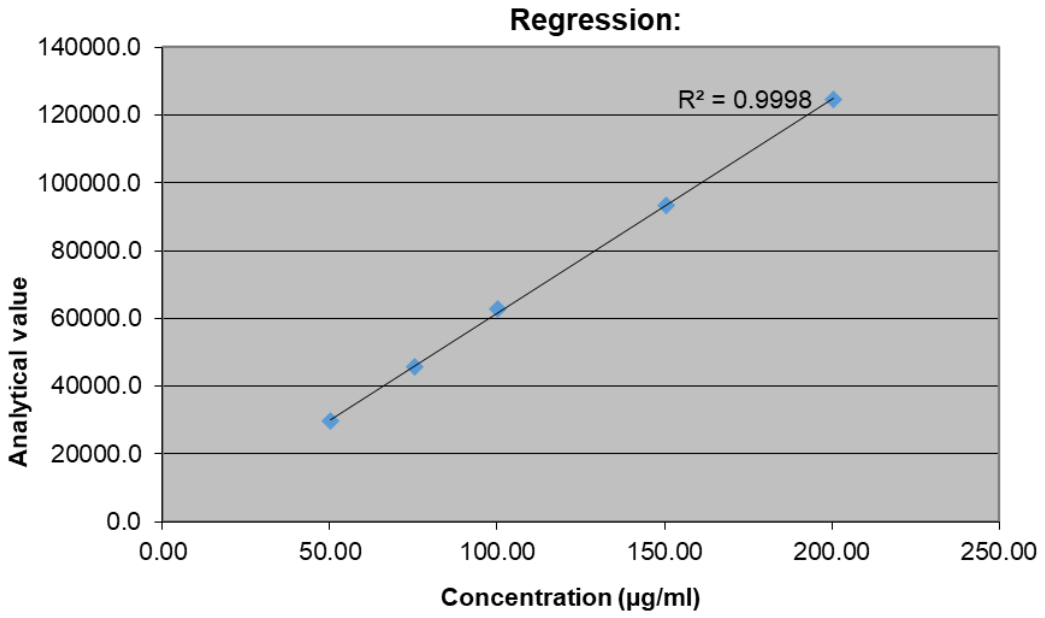

Figure 3.1: HPLC regression line obtained during method validation.

3.5 Conclusion

A validated and published HPLC method was used for the analysis of the artesunate (ART) recrystallisation products during this investigation.

All of the known solid-state techniques were employed in this study to characterise and identify possible new solid-state forms of ART raw material. The analytical results are presented and discussed in Chapter 4.

References

Anon. 2019. Leica KL200 LED. https://downloads.leica-microsystems.com/Leica%20KL200%20LED/Brochures/Leica_KL200LED-L2_Brochure_IT.pdf [Date of access: 18 July 2019].

Brown, M.E. 2001. Introduction to thermal analysis. Netherlands: Kluwer Academic Publishers, 264p.

Bernstein, J. 2002. Polymorphism in molecular crystals. Oxford: Clarendon Press. 410p.

International Pharmacopoeia. 2017. 7th *ed*. http://apps.who.int/phint/pdf/b/Jb.6.1.34.pdf [Date of access: 16 July 2018].

Ph. Int. *see* International Pharmacopoeia.

Rodriguez-Spong, B., Price, C.P., Jayasankar, A., Matzger, A.J. & Rodriguez-Hornedo, N. 2004. General principles of pharmaceutical solid polymorphism: a supramolecular perspective. *Advanced Drug Delivery Reviews*, 56(3): 241-274.

Chapter 4

Solid-state forms of artesunate

4.1 Introduction

Single X-ray diffractometry is commonly used for the determination of the unit cells of a crystal, while also providing accurate cell dimensions and the positions of the atoms within the crystal lattice. This technique is therefore ideal for determining whether a new solid-state form (polymorphic form and/or solvate) of an entity had been formed.

The Cambridge crystallographic data centre (CCDC) is a highly recommended and comprehensive source of reported structures. Structures that have been identified and characterised by researchers, for example, can be uploaded to the CCDC, from where they are then available to interested parties, such as researchers and manufacturers. During this study, therefore, the CCDC was searched for any existing entries referring to artesunate (ART) crystal forms. Four entries were found, with reference codes FAHFAV, FAHFAV01, FAHFAV02 and MEXKOP (as cited by Caira, 2019). Three of these entries, i.e. FAHFAV, FAHFAV01 and FAHFAV02 (Form 1) are of the same crystalline phase and represent the raw material that is currently commercially available (stereoisomer 10-α-artesunate; orthorhombic with space group $P2_12_12_1$). MEXKOP was found to be the ß-isomer of ART (as cited by Caira, 2019).

Lisgarten *et al*. (2002) also report that the crystals, recrystallised from methanol, are orthorhombic, with space group $P2_12_12_1$. They hence also represent the same form as the ART raw material (Form 1).

A recrystallisation study was conducted, aimed at finding a possibly new polymorphic form(s) of ART. The results are presented in this chapter.

4.2 Preparation of artesunate crystals

The recrystallisation process is discussed in Chapter 1. The solution should be super-saturated, after which first and second nucleation would occur (Byrn *et al.,* 1999).

Various super-saturated solutions of ART were prepared in glass beakers, by using different organic solvents. The beakers were sealed with parafilm® and the solvents allowed to evaporate at room temperature in an Asecos closed cabinet. This process is henceforward referred to as ‘slow recrystallisation’.

4.2.1 Slow recrystallisation method

Approximately 1 g of ART powder was added to glass beakers of various sizes, depending on the required volumes of the different solvents used to prepare the super-saturated solutions. The glass

beakers, containing the prepared solutions, were then sealed with a layer of parafilm and left undisturbed for a reasonable period of time in the closed cabinet, to allow for the evaporation of the solvents at room temperature. All crystal forms of ART were obtained by using the slow recrystallisation method. Table 3.1 (Chapter 3) summarises all the solvents and water dilutions used to yield the different recrystallisation products.

4.2.2 Classification of the recrystallised artesunate crystal forms

The physico-chemical properties of recrystallised ART crystals were consequently determined. According to the different solid-state techniques used in this study, such as X-ray powder diffractometry, infrared spectroscopy and thermal analysis, the crystals, resulting from the different solvents, could be classified into the three groups, i.e. Form 1 crystals, solvates, and new possible polymorphic forms, as discussed next.

4.2.2.1 Form 1

1. Artesunate (ART) raw material (FAHFAV, FAHFAV01, FAHFAV02) (Form I).
2. Crystals obtained from diethyl ether.
3. Crystals obtained from ethyl acetate.
4. Crystals obtained from tetrahydrofuran.
5. Crystals obtained from acetone (X-ray powder diffractograms similar to that of Form 1, but FT-IR spectra differed).
6. Crystals obtained from 1-butanol and 2-butanol.
7. Desolvation product from dichloromethane (DCM) solvate, i.e. DCM desolvate.

4.2.2.2 Solvate

1. DCM solvate (confirmed with single X-ray crystallography).

4.2.2.3 New possible polymorphic forms

1. Crystals obtained from acetonitrile (ACN).
2. Crystals obtained from acetone (most probably a solvate that had desolvated easily).
3. Crystals obtained from methanol (100%).
4. Identical physico-chemical properties obtained for crystals, recrystallised from ethanol and different ethanol:water mixtures, from 1-propanol, 2-propanol, and from methanol:water (50:50).

4.3 Characterisation of the artesunate raw material and prepared artesunate forms

4.3.1 X-ray powder diffractometry (XRPD)

The X-ray powder diffractometry tests were performed according to the method, described in Chapter 3 (par. 3.3.1.1). The complete data set of every XRPD determination is presented in Annexure A.

4.3.1.1 Form 1

The X-ray powder diffractograms of all the recrystallisation products that resemble that of Form 1, are illustrated in Figure 4.1. They include the ART raw material, the desolvation product from DCM solvate, as well as the crystals obtained from diethyl ether, ethyl acetate, tetrahydrofuran, acetone, 1-propanol, 1-butanol and 2-butanol.

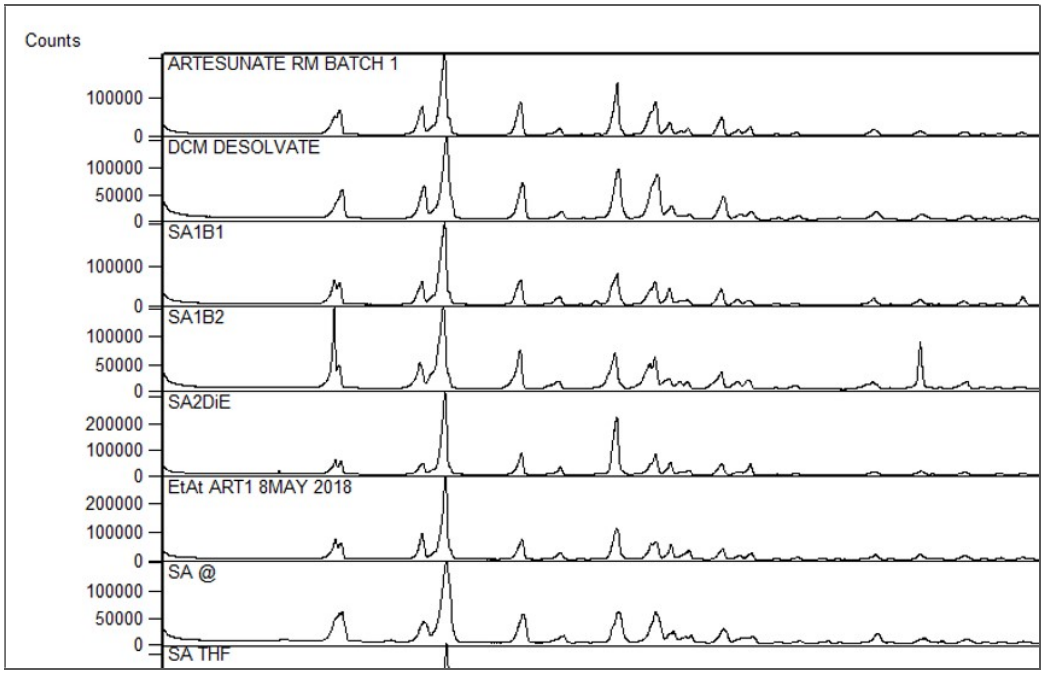

Figure 4.1: X-ray powder diffractograms, from top to bottom: ART raw material (Form 1), DCM desolvate, recrystallisation products (Form I) obtained from 1-butanol, 2-butanol, diethyl ether, ethyl acetate, acetone and tetrahydrofuran.

The peak intensity at 9.5°2Θ and 28.6°2Θ of the recrystallisation product obtained from 2-butanol (**SA1B2**), differed markedly from the other crystals' measurements. This could be attributed to the possible preferred orientation of the crystals.

4.3.1.2 Dichloromethane (DCM) solvate stability

Some of the X-ray powder diffractograms of the DCM solvate being measured at hourly intervals over a period of 24 h, are illustrated in Figure 4.2. The DCM crystals (obtained from slow recrystallisation), were cautiously ground while still submerged within the mother solvent, and covered with Kapton® film to minimise desolvation and possible structural changes during analysis. The sample was kept in the X-ray powder diffractometer instrument and measured hourly to observe any possible changes, or desolvation over a 24 h period. The results revealed that the DCM solvate was stable for approximately 5 h after the initial XRPD run. Complete desolvation was observed only after 24 h.

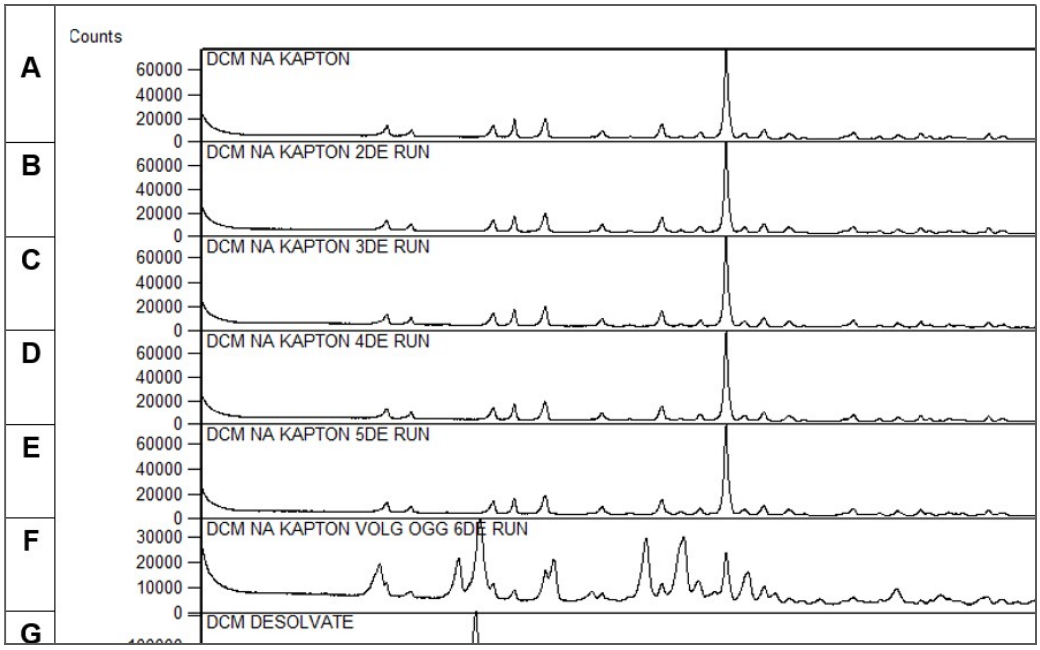

Figure 4.2: X-ray powder diffractograms of the DCM solvate, illustrating any possible occurrence of desolvation over a 24 h period. (A) First run, (B) after 1 h, (C) after 2 h, (D) after 4 h, (E) after 5 h, (F) after 6 h, and (G) complete desolvation after 24 h (transformed back into Form 1).

4.3.1.3 New possible polymorphic forms

1. The X-ray powder diffractograms of the possibly new polymorphic forms obtained during this study are illustrated in Figure 4.3. They include:
    a. Crystals obtained from ACN.
    b. Crystals obtained from methanol (100%).
    c. Identical physico-chemical properties obtained for crystals recrystallised from ethanol and different ethanol:water mixtures, from 1-propanol, 2-propanol and from methanol:water (50:50).

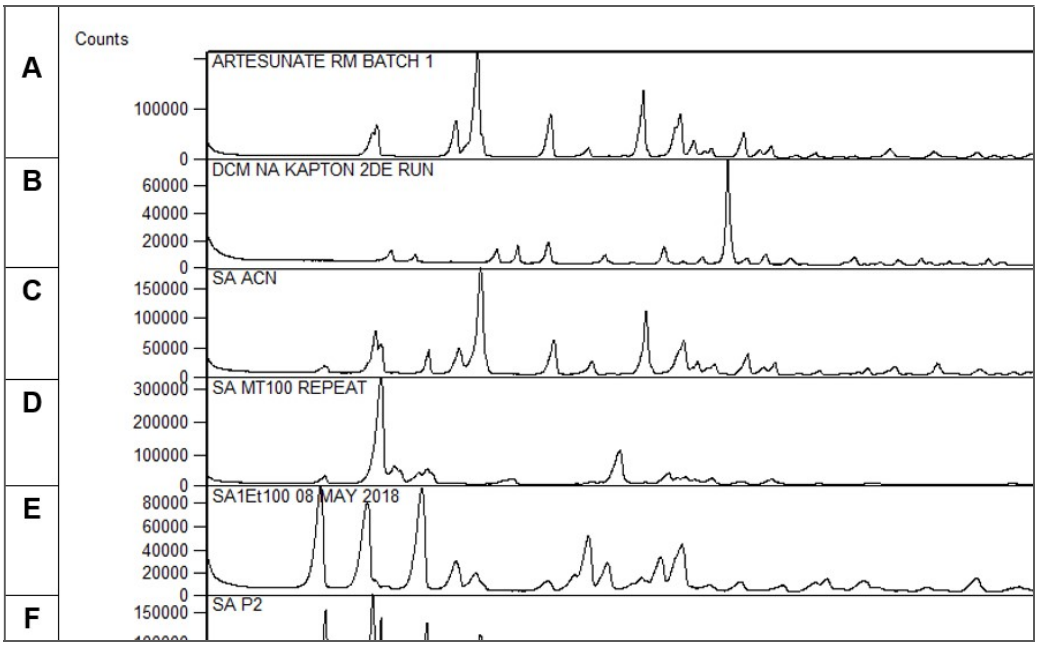

Figure 4.3: X-ray powder diffractograms of (A) ART raw material, (B) DCM solvate, recrystallisation products obtained from (C) ACN, (D) methanol, (E) ethanol (this diffractogram also represents recrystallisation products from methanol:water (50:50), 1-propanol, and (F) 2-propanol).

In Figure 4.4, the different recrystallisation products from the alcohols used in this study are illustrated. Significant differences were observed among the resultant products. The crystals obtained from methanol differed from those of Form 1 and also differed from the crystals obtained from the other alcohols. The crystals, prepared from ethanol, 1-propanol and 2-propanol, had similar XRPD patterns, but also differed from the other resulting products. Both the recrystallisation products from 1-butanol and 2-butanol were similar to Form 1.

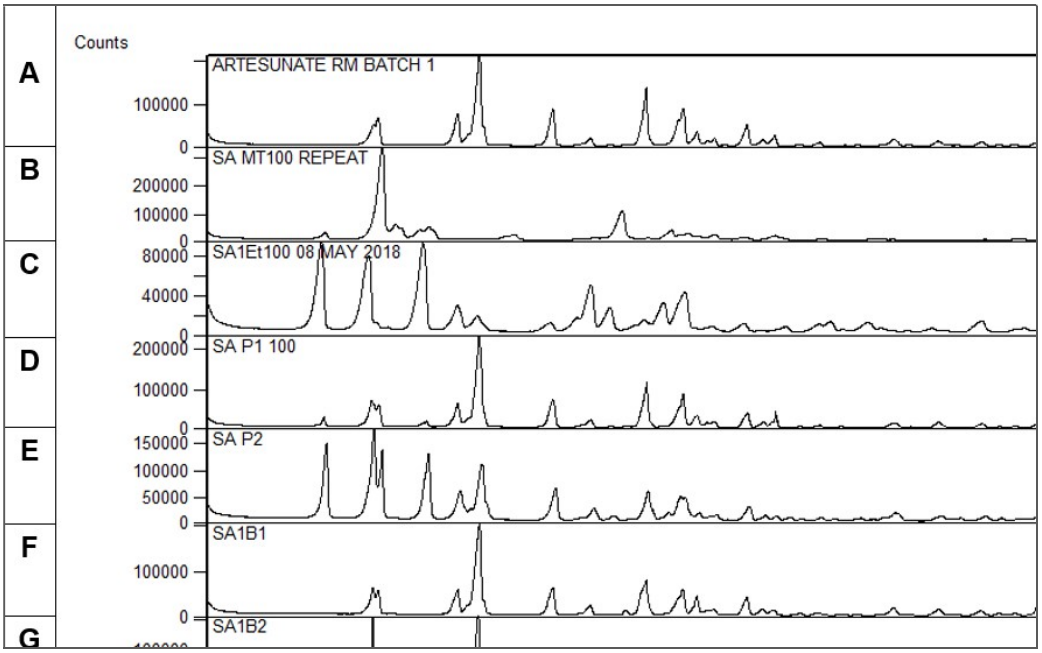

Figure 4.4: X-ray powder diffractograms of the recrystallisation products from the alcohol group. (A) ART raw material, (B) methanol, (C) ethanol, (D) 1-propanol, (E) 2-propanol, (F) 1-butanol and (G) 2-butanol.

In Figure 4.5, the recrystallisation products obtained from methanol and the different methanol:water mixtures are illustrated. As previously mentioned, the methanol recrystallisation product was dissimilar to Form 1. The recrystallisation products obtained from the mixtures of methanol and water did show some resemblance to those obtained from ethanol and propanol.

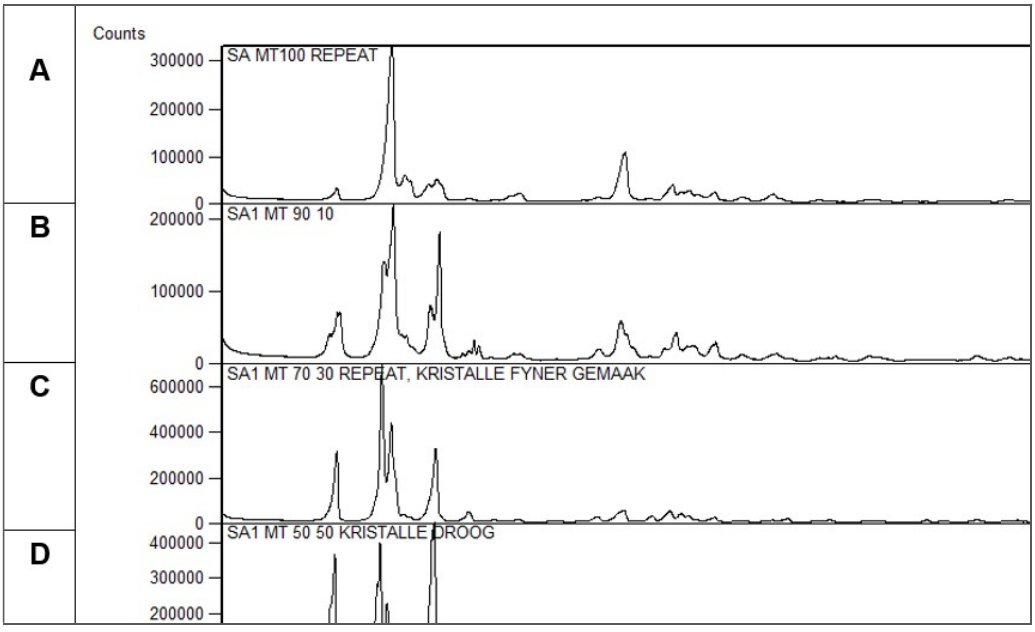

Figure 4.5: X-ray powder diffractograms of the recrystallisation products obtained from (A) methanol (100%), (B) methanol:water (90:10), (C) methanol:water (70:30), (D) methanol:water (50:50), illustrating possible preferential orientation of the crystals produced.

4.3.1.4 Discussion of the X-ray powder diffractometry results

The X-ray powder diffractograms of the crystals obtained from ACN showed some resemblance to Form I. The only observed difference was a peak measured at 12°2Θ, which was quite a significant difference. Single X-ray diffraction (SXRD) would confirm whether it was a new polymorphic form, or not.

The various ethanol:water mixtures did not deliver any new form, as was the case with ethanol, 1-propanol and 2-propanol. The main difference in comparison with Form 1 was observed in the 6 -12°2Θ region.

The X-ray powder diffractograms of the methanol recrystallisation products (Figure 4.5) showed preferential orientation, while the diffractogram of the methanol:water (50:50) recrystallisation product was similar to that prepared from ethanol. The crystals obtained from methanol (100%) showed differences from Form 1, but whether it was indeed a new polymorphic form, or only due to the preferred orientation of the crystals, would be confirmed with SXRD.

The only ART solvate was obtained from recrystallisation from DCM, as was confirmed by SXRD.

4.3.2 Single X-ray diffraction

Single X-ray diffraction analysis of the DCM solvate was performed by Caira (2019). The detailed report is found in Annexure B. Several crystals were tested for their diffraction qualities to optimise the quality of data collection. Eventually, a single crystal, with dimensions given in Table 1 (Annexure B), was cut from a larger crystal, while still submerged within the mother solvent to avoid solvent loss. X-ray data collection (48 h) was carried out on a Bruker Apex II Duo diffractometer, with the crystal being maintained under a nitrogen cold stream at 100(2) K. In Figure 4.6, those atoms that were involved in classical hydrogen bonding, are labelled. One of the two unique O-H···O hydrogen bonds is illustrated, namely that between the -COOH group of the ART molecule A and the pyranose oxygen atom O4B of ART molecule B. The geometrical details are: H-bond designation O8A-H8A···O4B, with O8A···O4B 2.805(5) Å and angle O8A-H8A···O4B 164°.

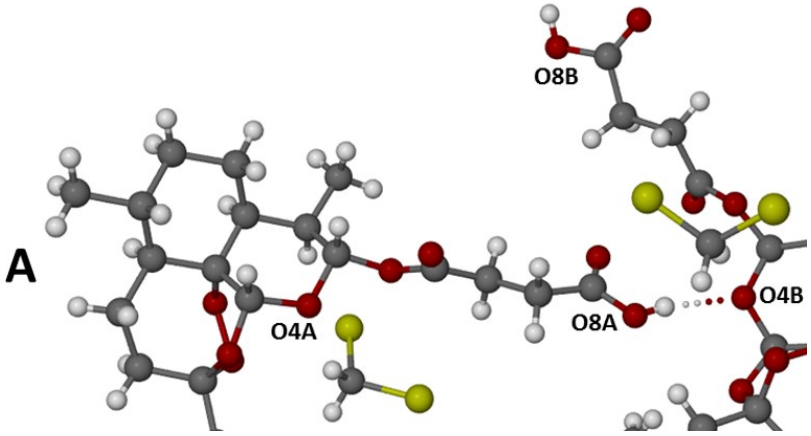

Figure 4.6: The asymmetric unit of the solvate, consisting of two independent ART molecules and three independent DCM molecules.

4.3.3 Fourier-transform infrared spectroscopy (FT-IR)

The FT-IR spectra were generated, as described in Chapter 3 (par. 3.3.4). The discussion of the FT-IR results follow below, at the end of par. 4.3.3.4 on page 47.

4.3.3.1 Form 1

The FT-IR spectra of all the recrystallisation products, which resemble that of Form 1, are illustrated in Figures 4.7 – 4.8, i.e. the ART raw material, the crystals obtained from diethyl ether, ethyl acetate, tetrahydrofuran, 1-butanol, 2-butanol and the desolvation product from DCM solvate. Two different batches of the ART raw material were analysed to test for the similarities (Form I).

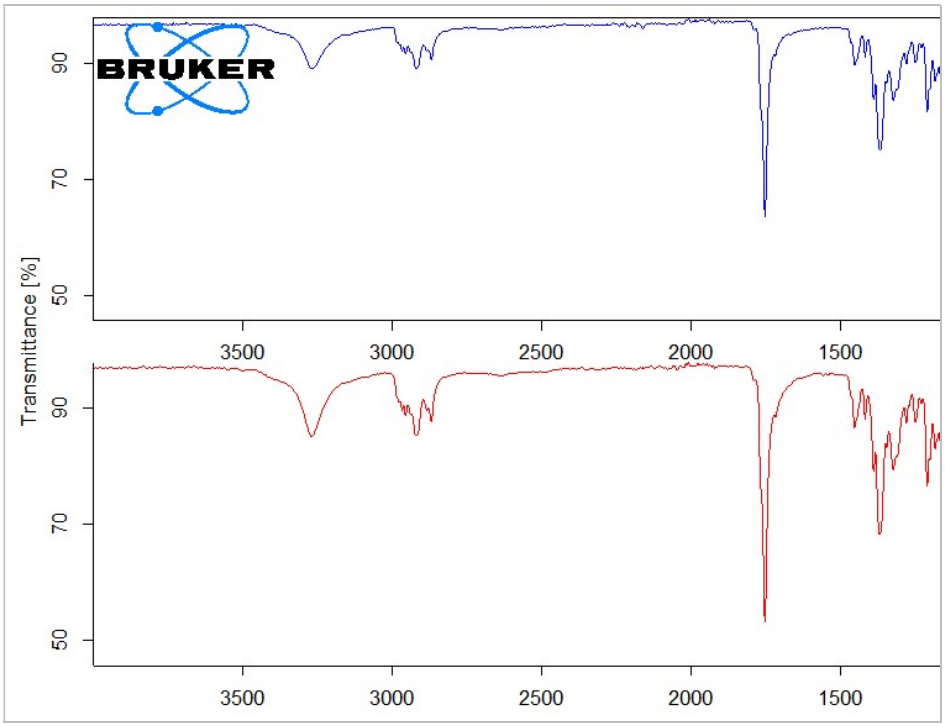

Figure 4.7: FT-IR spectra of two different batches of the ART raw material for a comparison of the similarities (Form I).

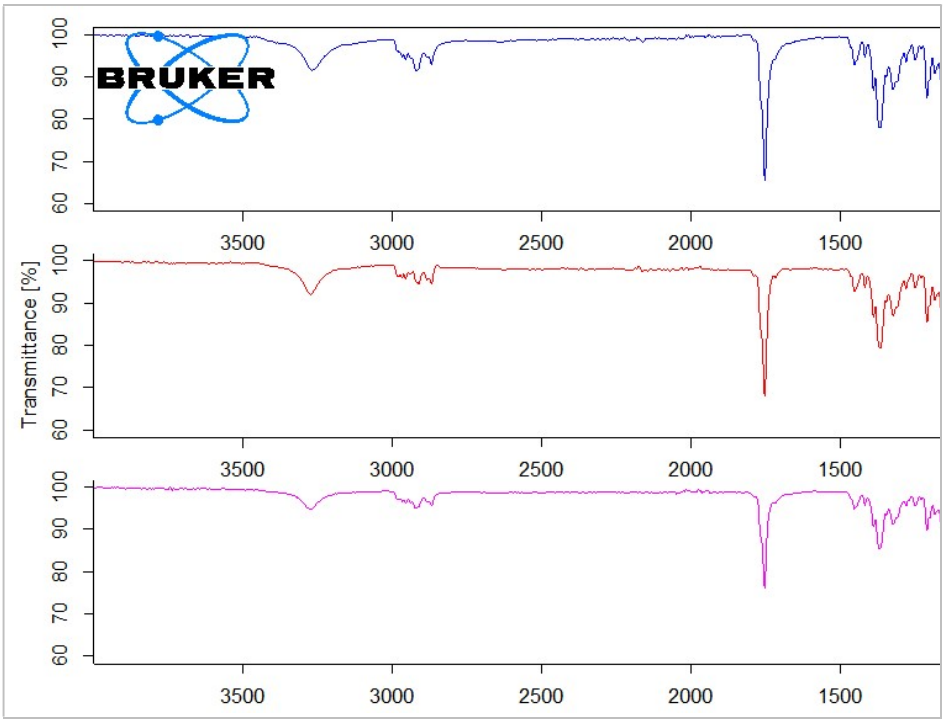

Figure 4.8: FT-IR spectra of the ART raw material (blue), DCM desolvation product (red) and recrystallisation product obtained from ethyl acetate (pink) (Form I).

All the FT-IR spectra of the recrystallisation products prepared from ethyl acetate, 1-butanol, 2-butanol, diethyl ether, tetrahydrofuran, as well as the DCM desolvate, displayed similar FT-IR spectra.

According to the XRPD results, the crystals from acetone were similar to Form 1, while their FT-IR spectra differed markedly. This could have been due to possible desolvation of the crystals during sample handling for the XRPD measurements. In Figure 4.10, the FT-IR spectra of the raw material (Form 1) and the recrystallisation product obtained from acetone illustrate these differences.

4.3.3.2 Dichloromethane solvate

In Figure 4.8, the FT-IR spectra of the DCM solvate and desolvate are illustrated.

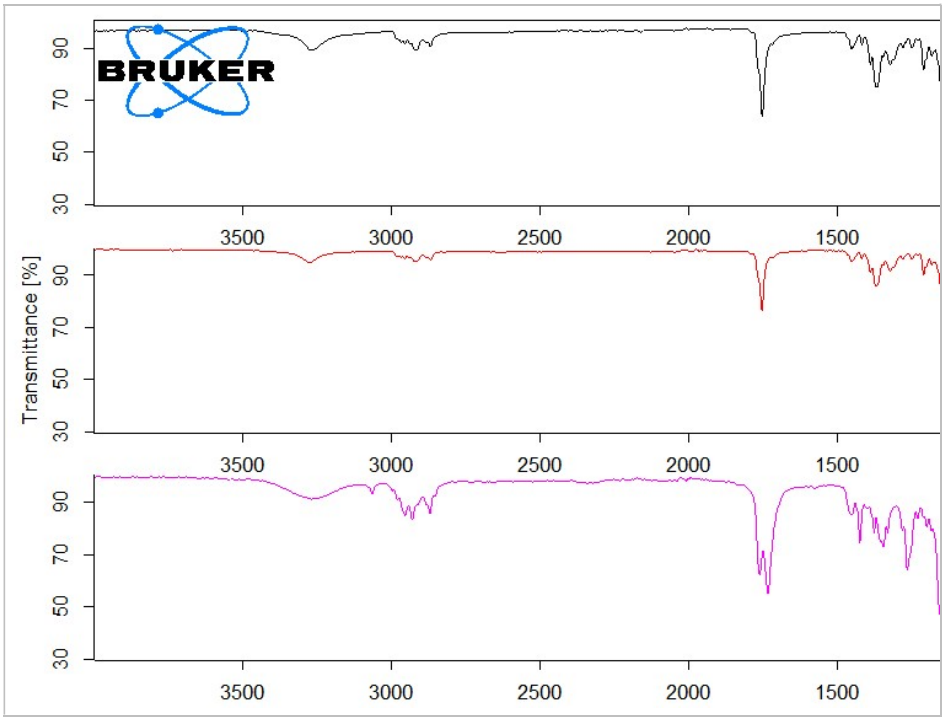

Figure 4.9: FT-IR spectra of the ART raw material (black), DCM desolvate (red) and DCM solvate crystals (pink).

As seen in Figure 4.9, the DCM solvate transformed back into Form 1 after desolvation. The FT-IR spectrum of the solvate, however, significantly differed from that of Form 1.

4.3.3.3 New possible polymorphic forms

1. The FT-IR spectra of all the possibly new polymorphic forms are illustrated in the following section.

    a. Crystals obtained from ACN (Figure 4.10).

b. Crystals obtained from acetone (Figure 4.11).

c. Crystals obtained from methanol (100%) (Figure 4.12).

d. Identical physico-chemical properties were obtained for crystals recrystallised from ethanol and different ethanol:water mixtures (Figure 4.16), 1-propanol and 2-propanol (Figure 4.14) and methanol:water (50:50).

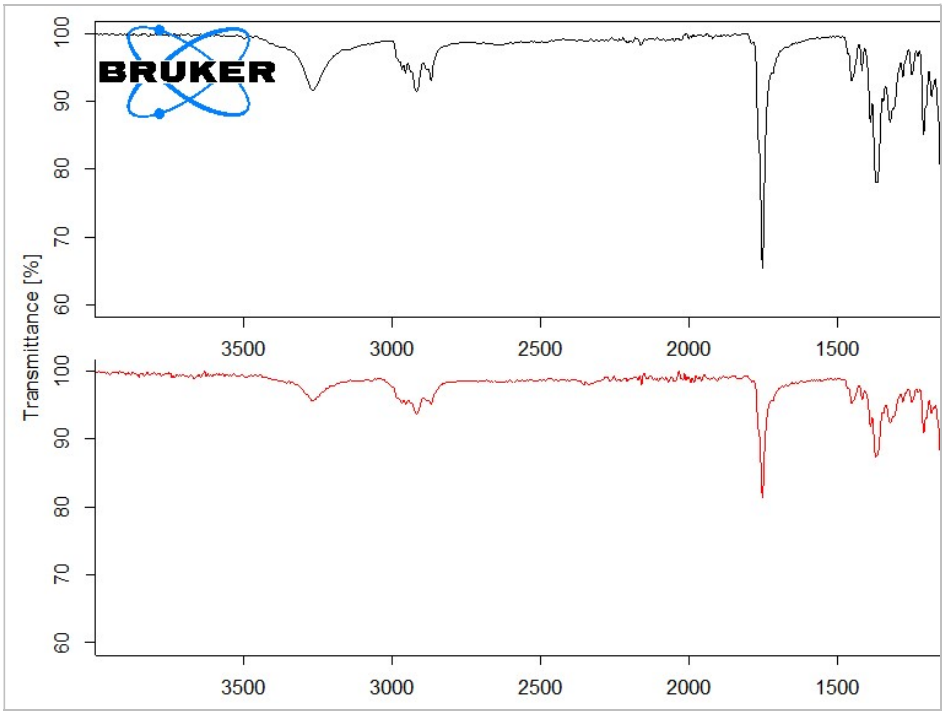

Figure 4.10: FT-IR spectra of the ART raw material (black) and the recrystallisation product from ACN (red).

The recrystallisation product of ACN showed some distinct differences in the XRPD measurements and was consequently classified as a possibly new polymorphic form. The FT-IR spectrum of ACN showed no significant differences when compared to that of the ART raw material. Further, studies should be done to confirm its status.

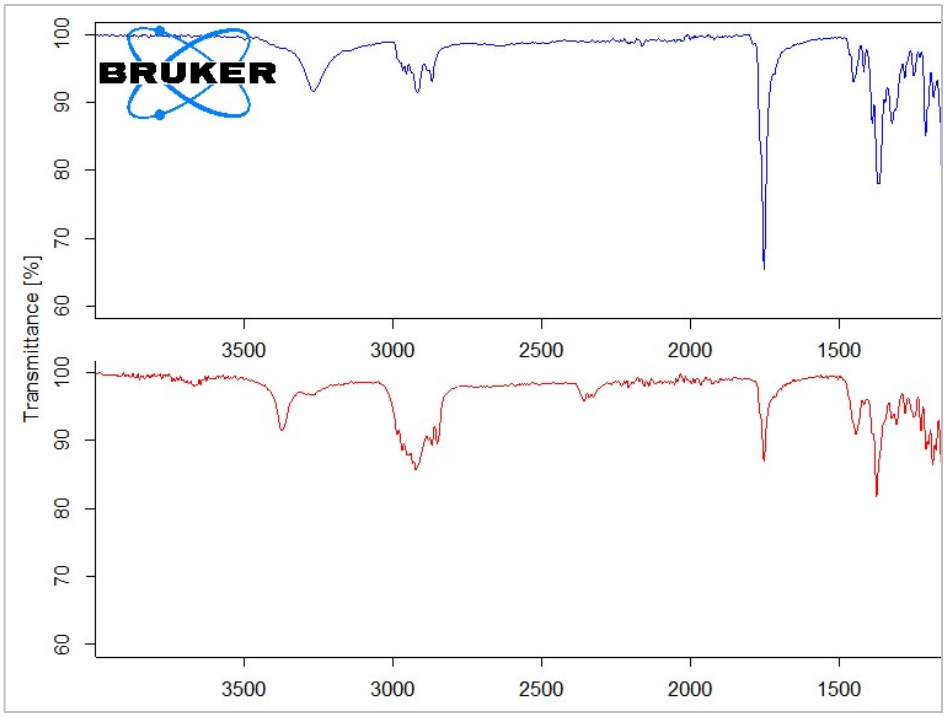

Figure 4.11: FT-IR spectra of the ART raw material (blue) and the recrystallisation product from acetone (red).

As mentioned earlier, the X-ray powder diffractogram of the acetone recrystallisation product showed no differences when compared to that of the ART raw material. The FT-IR spectrum, however, revealed a significant difference in the 3400-3200 cm^{-1} region. While the ART raw material had a peak at 3266 cm^{-1}, the acetone recrystallisation product had one at 3372 cm^{-1}.

A possible explanation for the discrepancy in results between the XRPD and FT-IR determinations could be that during the sample preparation for XRPD, which included grinding of the crystals to a fine powder, desolvation could have occurred and was the measurement therefore identical to that of the ART raw material.

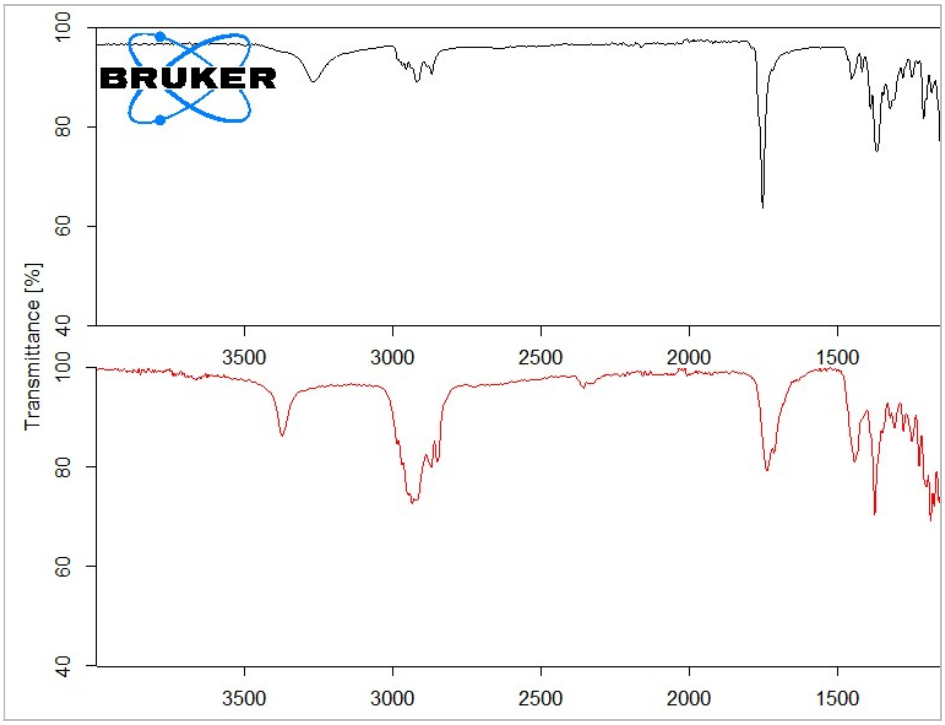

Figure 4.12: FT-IR spectra of the ART raw material (black) and the recrystallisation product from methanol (red).

The X-ray powder diffractogram showed that the recrystallisation product obtained from methanol (Figure 4.12) could possibly also represent a new polymorphic form. The FT-IR spectra obtained from the methanol and water mixtures were also similar to that of the methanol spectrum. The FT-IR spectrum of the crystals from methanol differed from that of the raw material. The methanol and methanol:water recrystallisation products displayed a peak at 3372 cm^{-1} in comparison with the 3266 cm^{-1} of Form 1 (ART raw material). This methanol recrystallisation product was further investigated and confirmed by SXRD.

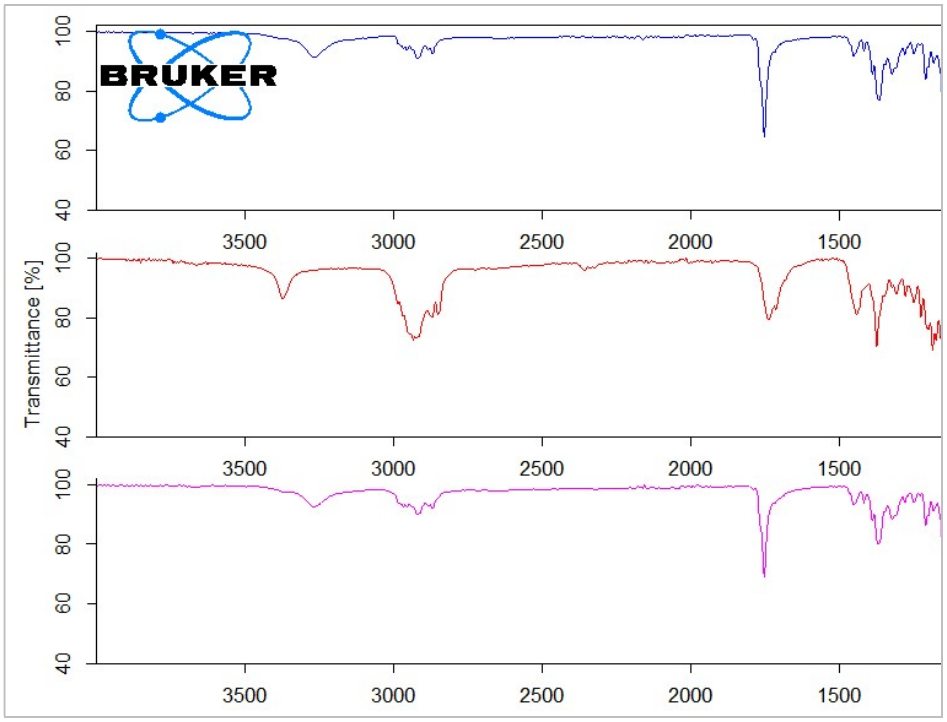

Figure 4.13: FT-IR spectra of the ART raw material (blue) and the recrystallisation products obtained from methanol (red) and the ethanol:water mixture (60:40) (pink).

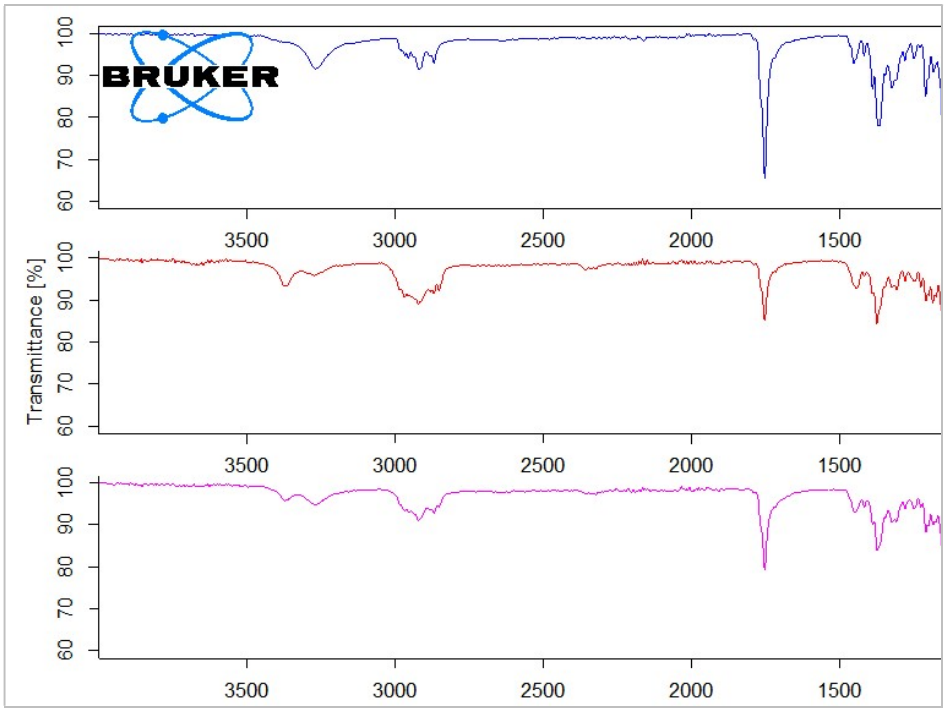

Figure 4.14: FT-IR spectra of the ART raw material (blue) and the recrystallisation products obtained from 1-propanol (red) and 2-propanol (pink).

The main difference in the spectra was again in the 3400-3200 cm^{-1} region. Both the 1-propanol and 2-propanol recrystallisation products displayed a peak at 3371 cm^{-1} in comparison with the the peak at 3266cm^{-1} of the ART raw material (Form 1).

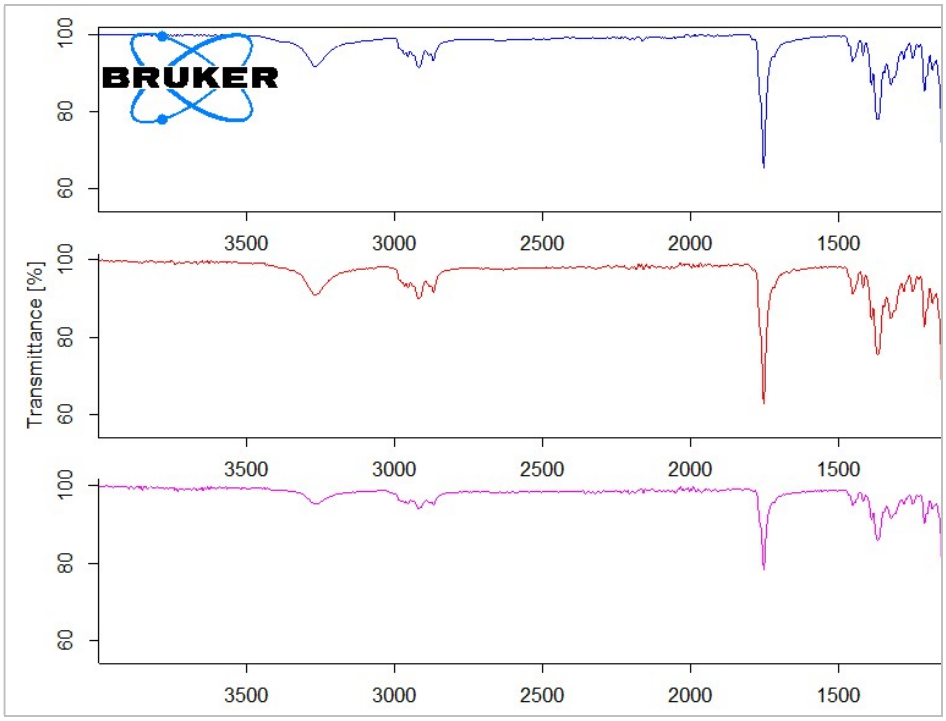

Figure 4.15: FT-IR spectra of the ART raw material (blue) and the recrystallisation products obtained from 1-butanol (red) and 2-butanol (pink).

The FT-IR spectra of all the butanol recrystallisation products were identical to that of the ART raw material, but differed from those of the products prepared from methanol, ethanol and propanol.

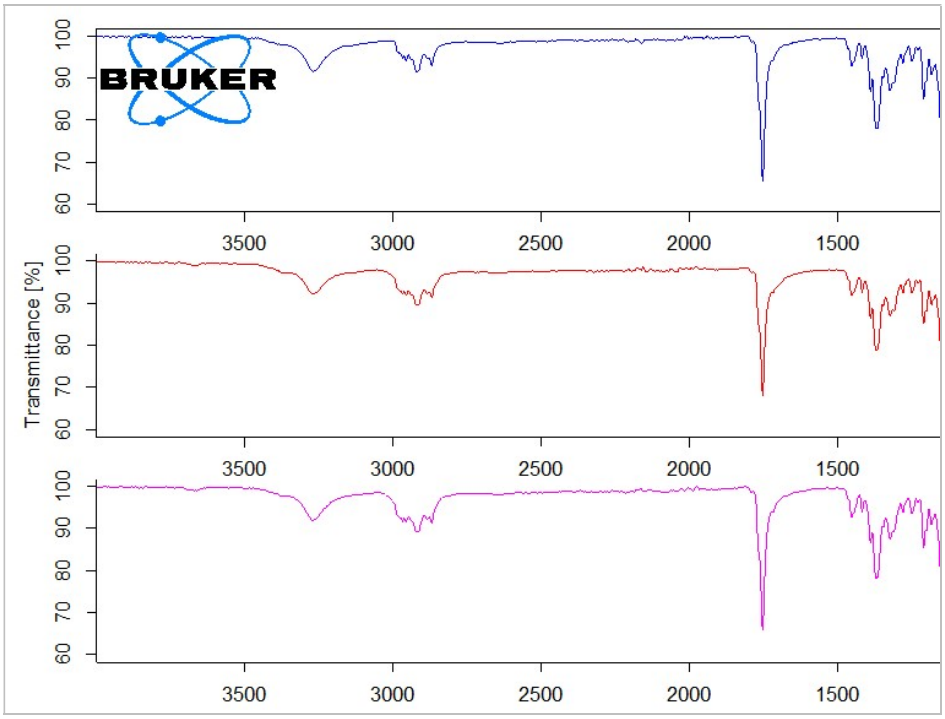

Figure 4.16: FT-IR spectra of the ART raw material (blue) and the recrystallisation products obtained from ethanol:water (60:40) (red) and ethanol:water (80:20) (pink).

For simplicity, only the ethanol:water mixtures in the ratios, (60:40) and (80:20), are displayed. All the ethanol:water mixtures produced crystals that were identical to those prepared from ethanol (100%).

Interestingly, the FT-IR spectra of the ethanol and ethanol:water mixtures were identical to that of the ART raw material. The X-ray powder diffractograms, however, showed some distinct differences. This occurrence should be further investigated in another study.

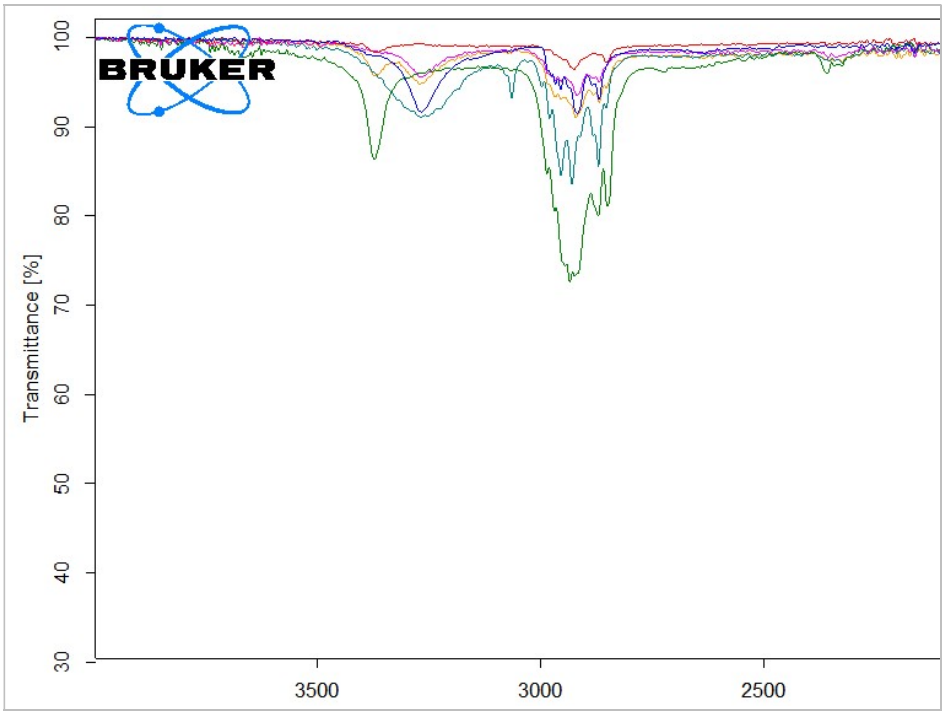

Figure 4.17: FT-IR overlay of the ART raw material (blue), and recrystallisation products obtained from ethanol (orange), ACN (pink), methanol (green), DCM solvate (cyan blue) and from 2-propanol (yellow).

In Figure 4.17, an overlay of the FT-IR spectra is shown, with some of the recrystallisation products prepared from DCM solvate, methanol, ethanol, 2-propanol and ACN. This overlay reveals some distinct differences between the ART raw material and the recrystallisation products.

4.3.3.4 Discussion of the FT-IR results

The FT-IR spectra were unfortunately not absolutely conclusive regarding the definite occurrence of different polymorphic forms, or possible polymorphic forms, as expected. Significant differences were, however, observed, as per the summarised spectral data in Table 4.3. FT-IR should not be used in isolation for the characterisation of the different ART solid-state forms.

Table 4.3: Some of the characteristic FT-IR absorption bands of the different recrystallisation products, compared to ART (Form 1)

Crystals	FT-IR absorption bands												
ART		3266				2918			1752			1369	

DCM solvate		3268	3064	2929		2929			1762				1154
DCM desolvate		3274		2955		2921	2867		1753			1370	1146
ACN		3269		2966		2919	2868		1752		1389		1145
Methanol	3372			2934			2850		1738	1443		1371	1100
Ethanol		3270		2920			2868		1753				1001
1-Propanol	3371	3271		2921				2356	1753		1390		1144
2-Propanol	3371	3271		2921					1752			1374	1145
1-Butanol		3269		2918			2868		1752			1369	1145
2-Butanol		3260		2966	2955		2867		1752			1369	1145
Diethylether		3272					2868		1754			1370	1146
EtAt		3273		2976		2910	2868		1753		1389		1145
Acetone	3374					2922		2357	1753			1375	1133
THF		3269		2966		2917	2867		1752			1364	1210

4.3.4 Simultaneous thermal analysis (STA)

The simultaneous thermal analysis procedures were performed under exact conditions and heating rates, as discussed in Chapter 3 (par. 3.3.2).

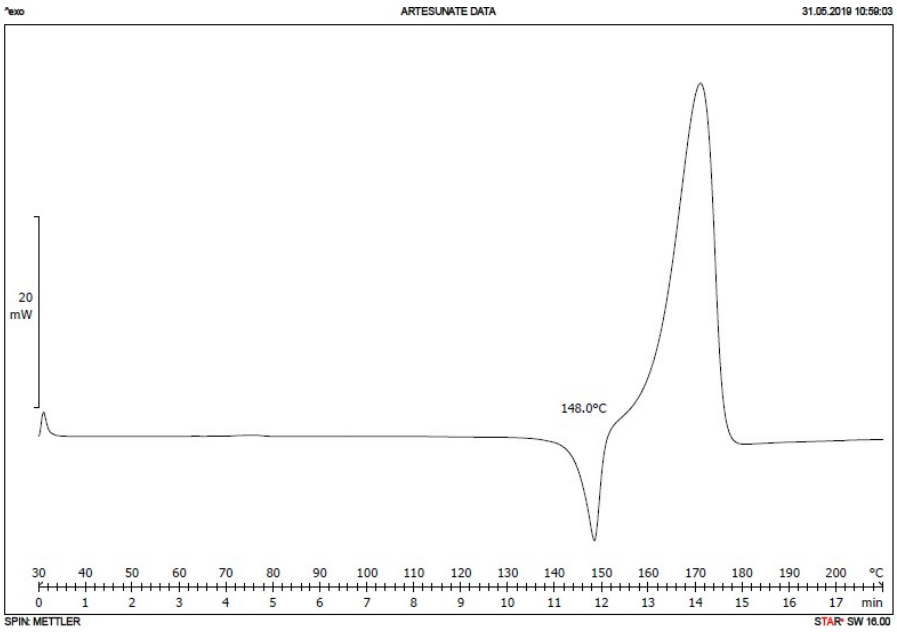

Figure 4.18: STA thermogram of the ART raw material, showing melting with decomposition at 146°C.

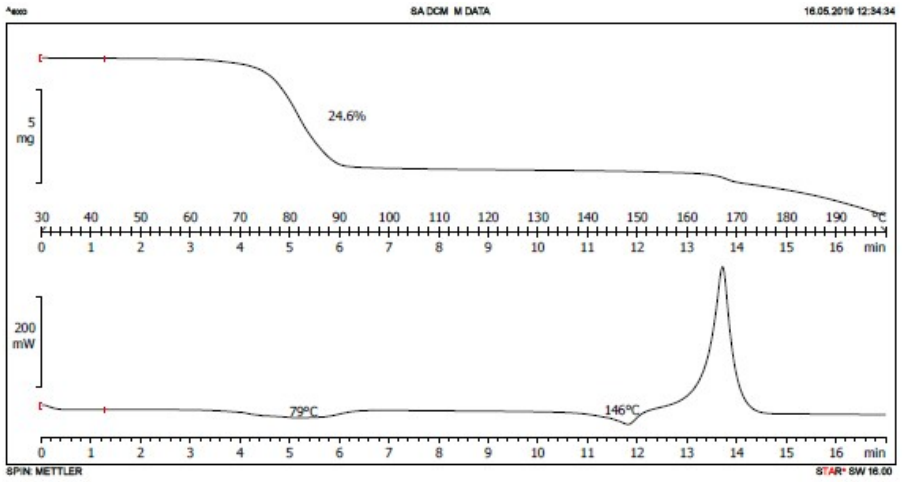

Figure 4.19: STA thermograms of the DCM solvate (Top: TGA, Bottom: DSC). TGA showed a 24.6% mass loss for the solvate.

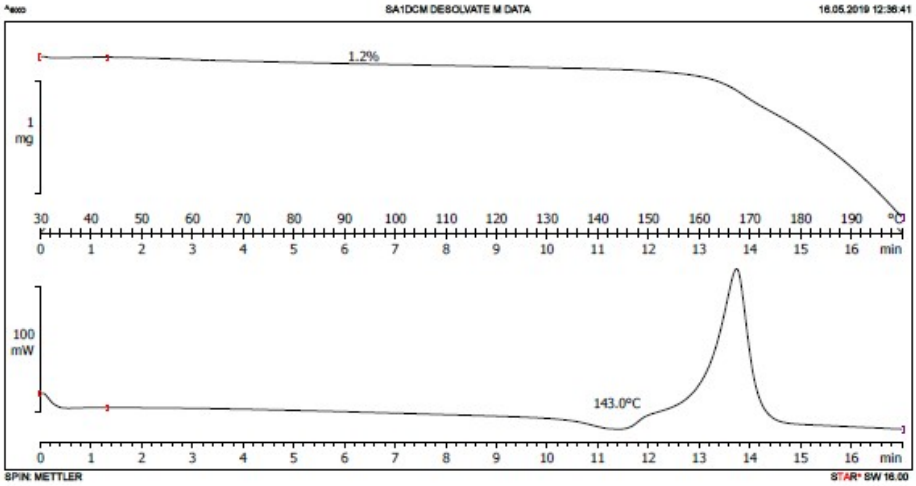

Figure 4.20: STA thermogram of the DCM desolvated crystals (Top: TGA, Bottom: DSC). No mass loss was recorded, as expected.

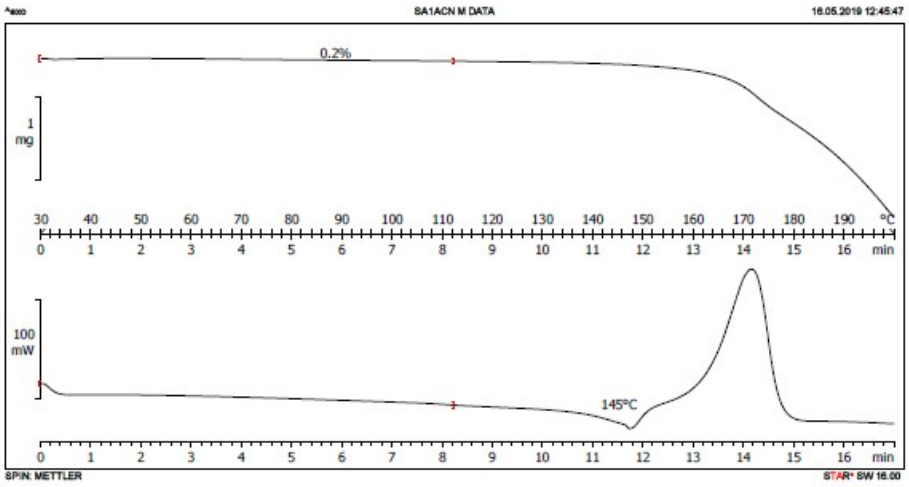

Figure 4.21: STA thermograms of the recrystallisation product obtained from ACN (Top: TGA, Bottom: DSC). No mass loss was recorded.

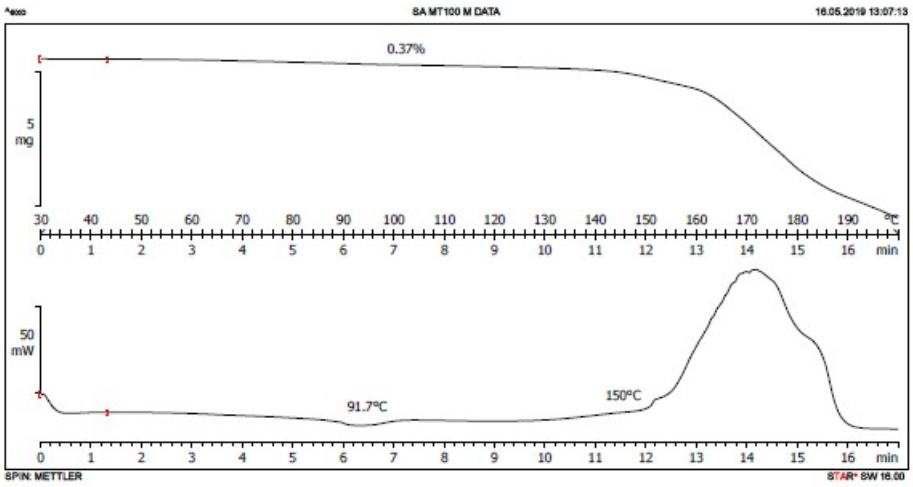

Figure 4.22: STA thermograms of the recrystallisation product obtained from methanol (Top: TGA, Bottom: DSC). No mass loss was recorded.

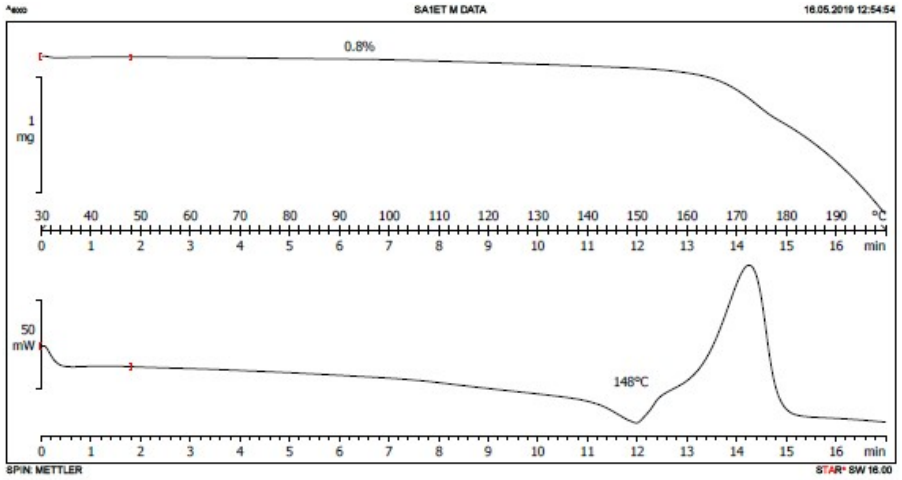

Figure 4.23: STA thermograms of the recrystallisation product obtained from ethanol (Top: TGA, Bottom: DSC). No mass loss was recorded.

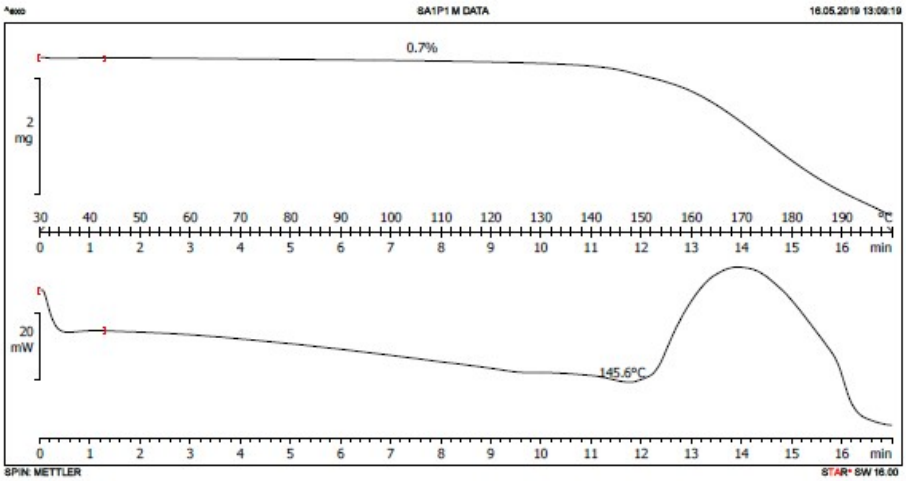

Figure 4.24: STA thermograms of the recrystallisation product obtained from 1-propanol (Top: TGA, Bottom: DSC). No mass loss was recorded.

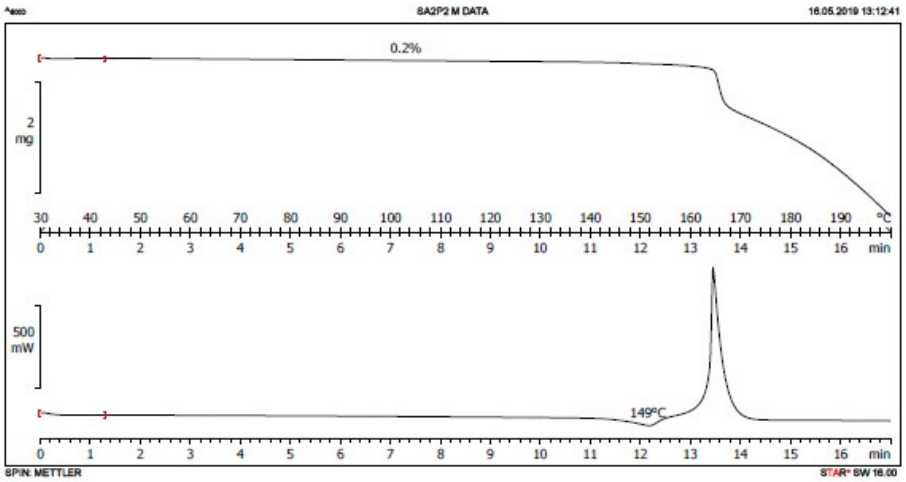

Figure 4.25: STA thermograms of the recrystallisation product obtained from 2-propanol (Top: TGA, Bottom: DSC). No mass loss was recorded.

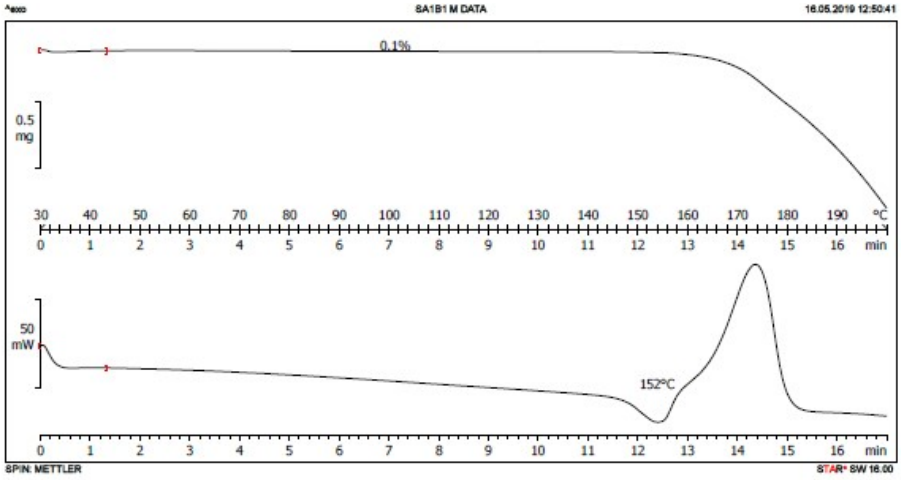

Figure 4.26: STA thermograms of the recrystallisation product obtained from 1-butanol (Top: TGA Bottom: DSC). No mass loss was recorded.

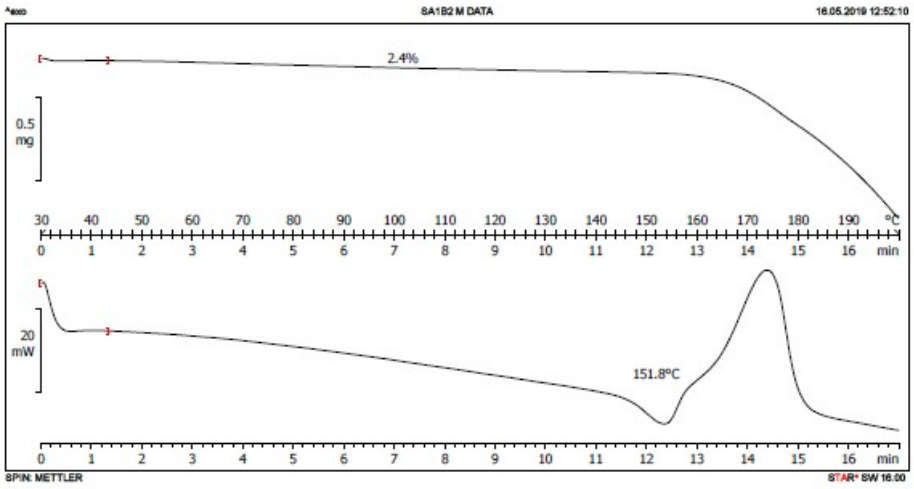

Figure 4.27: STA thermograms of the recrystallisation product obtained from 2-butanol (Top: TGA, Bottom: DSC). No mass loss was recorded.

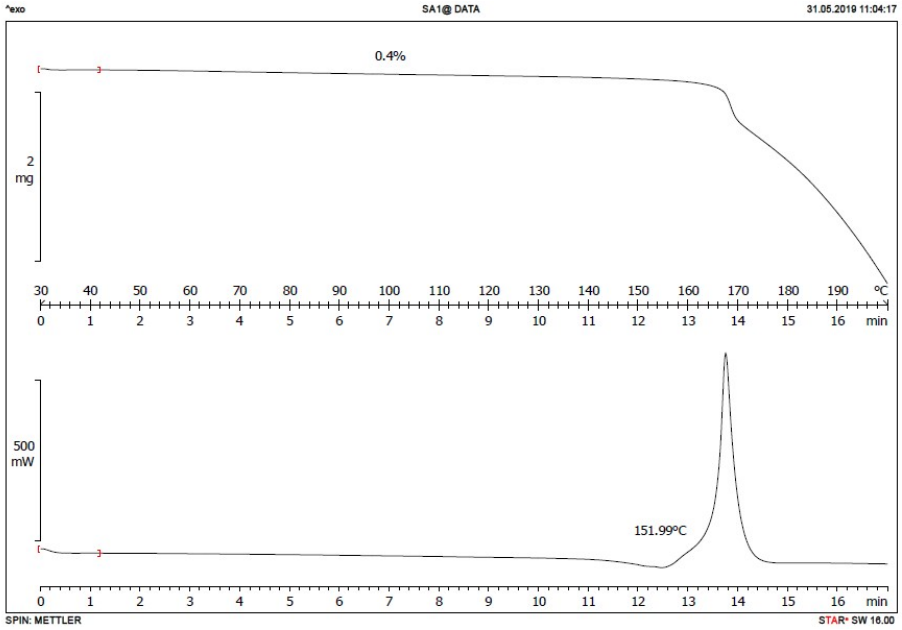

Figure 4.28: STA thermograms of the recrystallisation product obtained from acetone (Top: TGA Bottom: DSC). No mass loss was recorded.

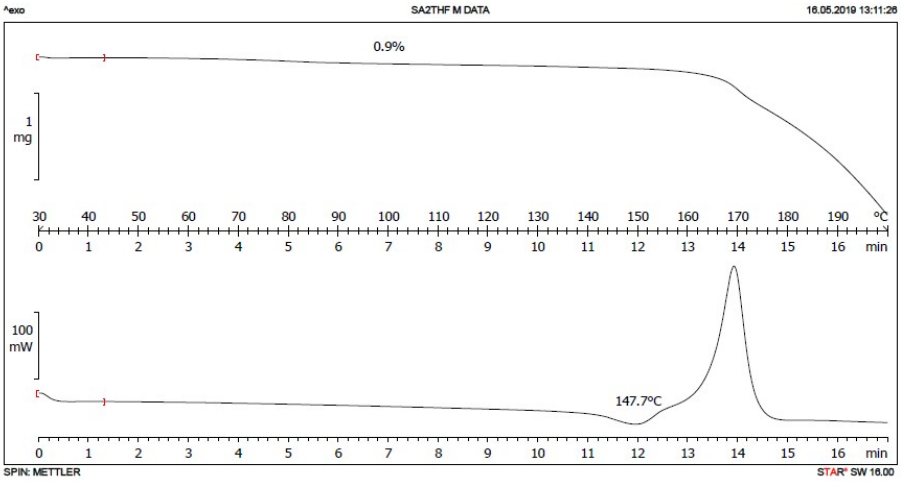

Figure 4.29: STA thermograms of the recrystallisation product obtained from tetrahydrofuran (Top: TGA, Bottom: DSC). No mass loss was recorded.

4.3.4.1 Discussion of the thermal analysis results

The theoretical mass loss being calculated for a DCM:ART (1:1) solvate was 18%. The value obtained for the DCM solvate was on average 24.6%, thereby suggesting an ART:DCM (2:3) solvate. This was confirmed with a single X-ray crystallographic study (Annexure B).

All the forms and recrystallisation products showed a minimal mass loss, as calculated with the TGA software, suggesting that only DCM produced a solvate. The melting points of the different recrystallisation products and mass losses are presented in Table 4.4.

Table 4.4: Results of the STA analyses

Form	Peak maximum (°C)	% Theoretical mass loss calculated for a 1:1 solvate	Mass loss (%)
ART raw material	148	N/A	0
DCM solvate	146	18	24.6
DCM desolvate	143	N/A	1.2
ACN	145	9.66	0.2
Methanol	150	7.7	0.37
Ethanol	148	10.71	0.5
1-Propanol	146	13.53	0.7
2-Propanol	149	13.53	0.2
1-Butanol	152	16.18	0.1
2-Butanol	152	16.18	2.4
Diethylether	155	16.18	1

Ethyl acetate	155	18.66	0.8
Acetone	152	13.14	0.4
Tetrahydrofuran	148	15.81	0.9

4.3.5 Powder dissolution

A VanKel700 (Varian, USA) dissolution bath was used for powder dissolution testing. USP apparatus 2 (paddle) was set up at 37°C at a rotational speed of 100 rpm, using 1000 mL dissolution vessels. The experiments were performed with distilled water (900 mL) as the dissolution medium. The experimental set-up is described in Chapter 3 (par. 3.3.5).

Table 4.5: Powder dissolution results of the ART raw material

Powder dissolution: ART raw material (µg/ml)								
Vessel	**Vortex time intervals**	**5 min**	**10 min**	**20 min**	**30 min**	**60 min**	**120 min**	**180 min**
1	0 min	0	0	12.22	15.62	20.58	19.97	14.51
2	2 min	0	12.79	16.10	17.40	19.22	17.88	14.15
3	4 min	0	0	15.69	14.43	16.56	20.04	14.08
4	6 min	0	18.66	20.70	14.72	27.14	19.71	16.29
5	8 min	0	12.39	19.97	25.65	26.76	20.37	22.62
6	10 min	0	15.47	19.42	20.14	25.69	22.05	24.07
	Average (µg/ml)	**0**	**9.89**	**17.35**	**17.99**	**22.66**	**20.01**	**17.62**

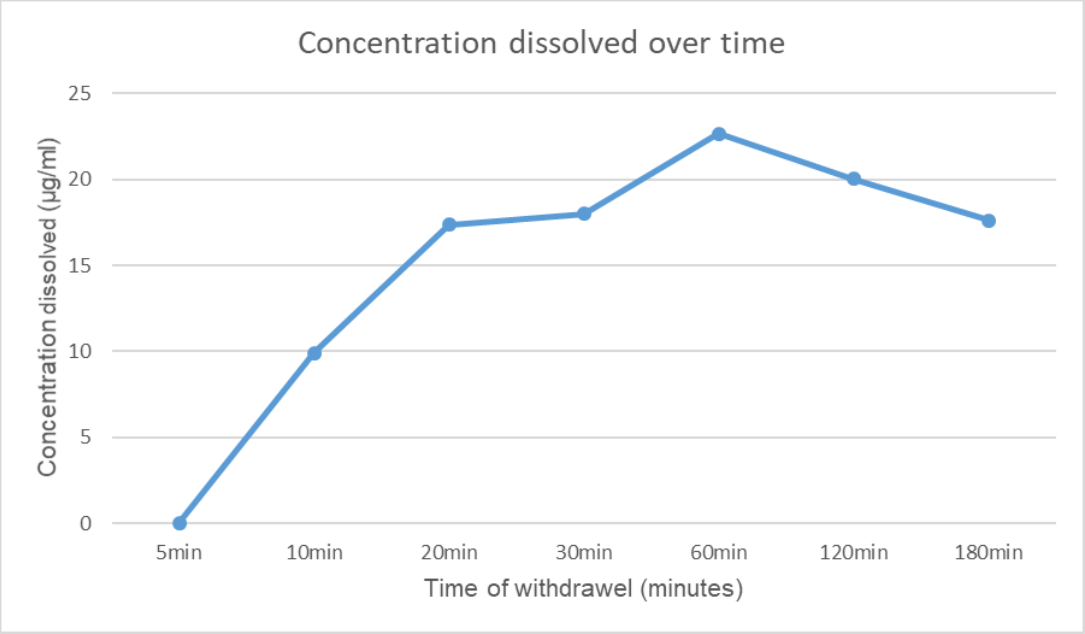

Figure 4.30: Powder dissolution profile of the ART raw material.

Table 4.6: Powder dissolution results of the DCM solvate crystals

Powder dissolution: DCM solvate crystals (µg/ml)								
Vessel	**Vortex time intervals**	**5 min**	**10 min**	**20 min**	**30 min**	**60 min**	**120 min**	**180 min**
1	0 min	0	6.22	5.91	6.40	6.54	5.94	7.32
2	2 min	0	8.65	7.66	10.58	10.58	10.90	9.16
3	4 min	0	7.85	7.33	13.46	13.46	11.13	11.89
4	6 min	0	11.71	12.31	10.81	10.81	11.41	15.45
5	8 min	0	9.40	8.39	12.88	12.88	10.62	15.78
6	10 min	0	14.50	0	10.05	10.05	11.88	13.49
	Average (µg/ml)	**0**	**9.72**	**6.93**	**8.53**	**10.72**	**10.31**	**12.18**

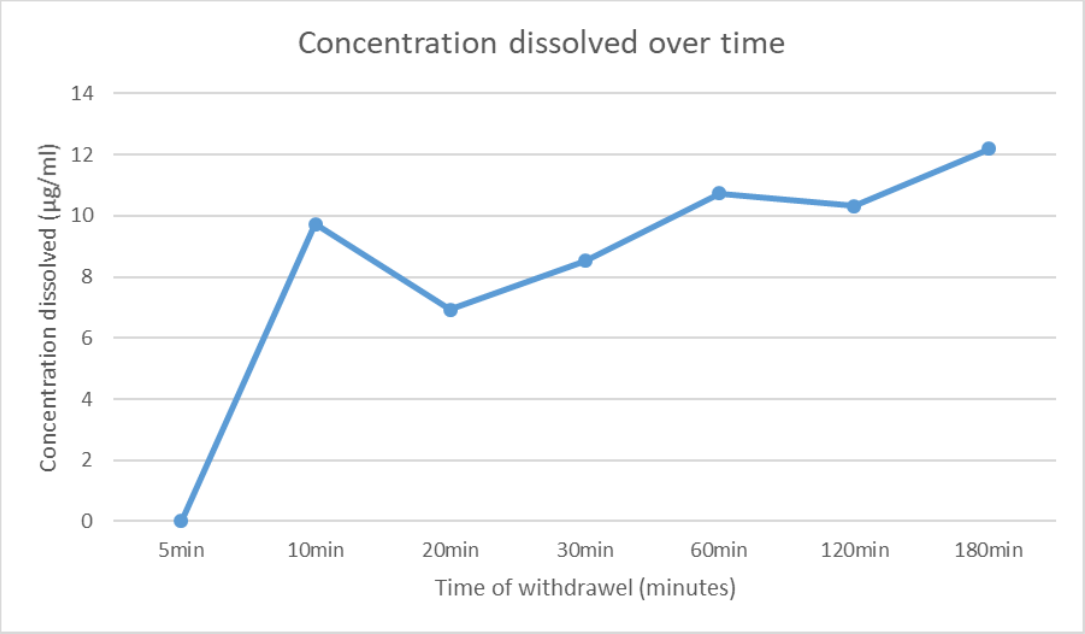

Figure 4.31: Powder dissolution profile of the DCM solvate crystals.

Table 4.7: Powder dissolution results of the DCM desolvated crystals

Powder dissolution: DCM desolvated crystals (µg/ml)								
Vessel	**Vortex time intervals**	**5 min**	**10 min**	**20 min**	**30 min**	**60 min**	**120 min**	**180 min**
1	0 min	0	18.48	27.29	33.22	40.51	42.03	35.64
2	2 min	0	18.06	23.97	31.55	37.46	37.64	35.76
3	4 min	0	17.47	22.89	31.43	35.15	37.20	31.98
4	6 min	0	19.57	27.60	32.04	38.08	38.04	34.76
5	8 min	0	19.69	25.54	30.00	32.46	32.21	24.84
6	10 min	0	19.22	27.09	33.30	37.90	39.24	31.46
	Average (µg/ml)	**0**	**18.75**	**25.73**	**31.92**	**36.93**	**37.73**	**32.41**

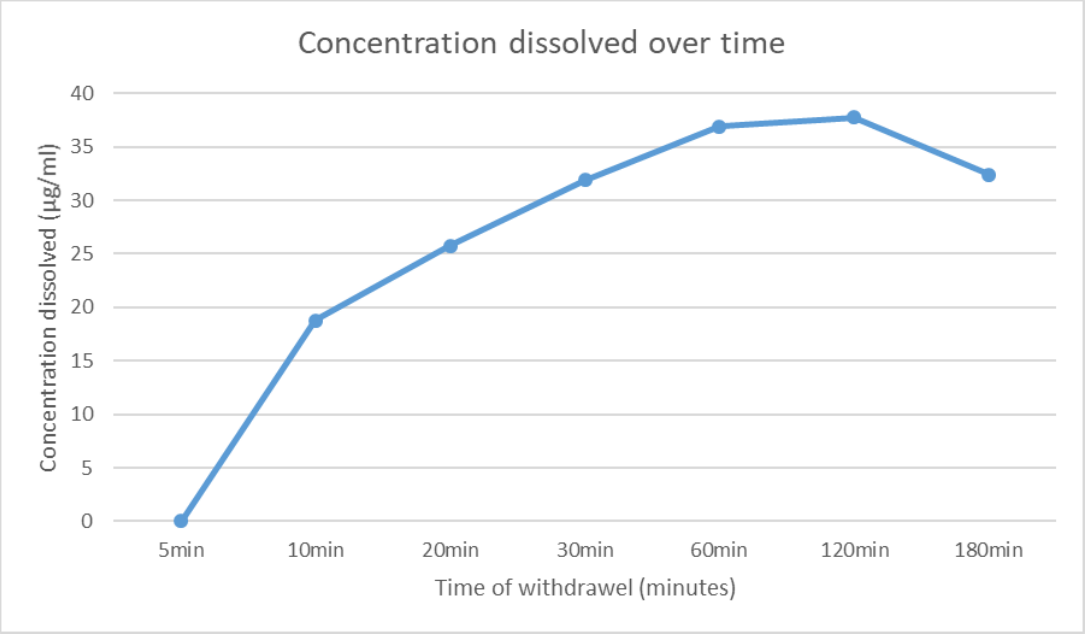

Figure 4.32: Powder dissolution profile of the DCM desolvated crystals.

Table 4.8: Powder dissolution results of the ethanol:water (60:40) crystals

Powder dissolution: Ethanol:water (60:40) crystals (µg/ml)								
Vessel	**Vortex time intervals**	**5 min**	**10 min**	**20 min**	**30 min**	**60 min**	**120 min**	**180 min**
1	0 min	0	4.75	5.26	5.11	6.28	6.02	3.15
2	2 min	0	5.39	7.62	8.76	9.06	3.29	4.22
3	4 min	0	3.18	4.55	6.59	8.26	4.14	4.94
4	6 min	3.29	5.02	5.61	7.17	6.58	5.65	4.94
5	8 min	0	6.08	5.77	6.02	5.57	5.75	4.92
6	10 min	3.48	3.10	5.23	5.20	6.45	6.91	3.87
	Average (µg/ml)	**1.13**	**4.59**	**5.67**	**6.47**	**7.03**	**5.29**	**4.34**

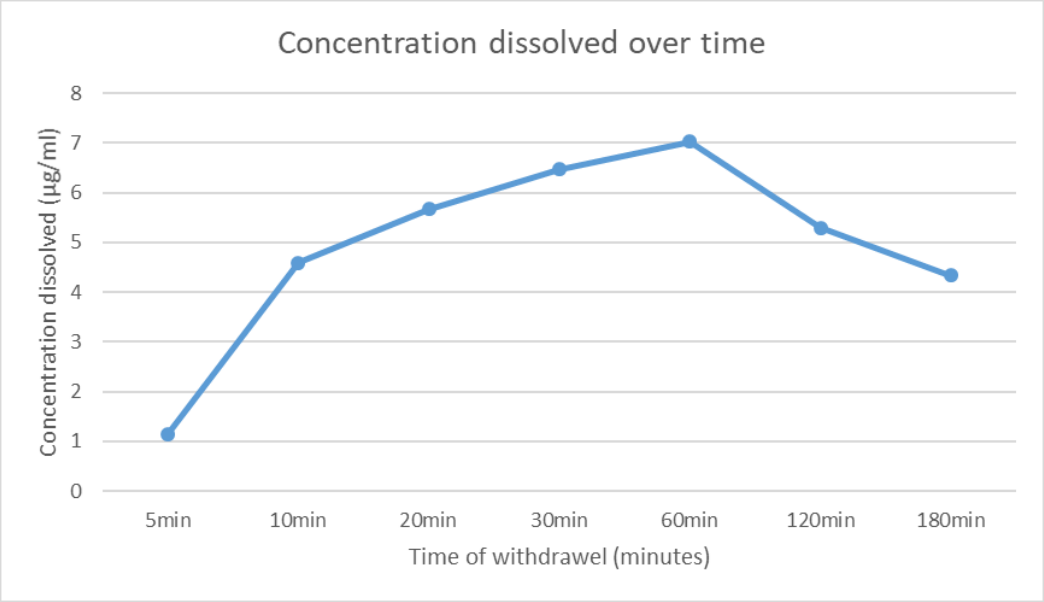

Figure 4.33: Powder dissolution profile of the crystals obtained from ethanol:water (60:40).

4.3.5.1 Discussion of the powder dissolution results

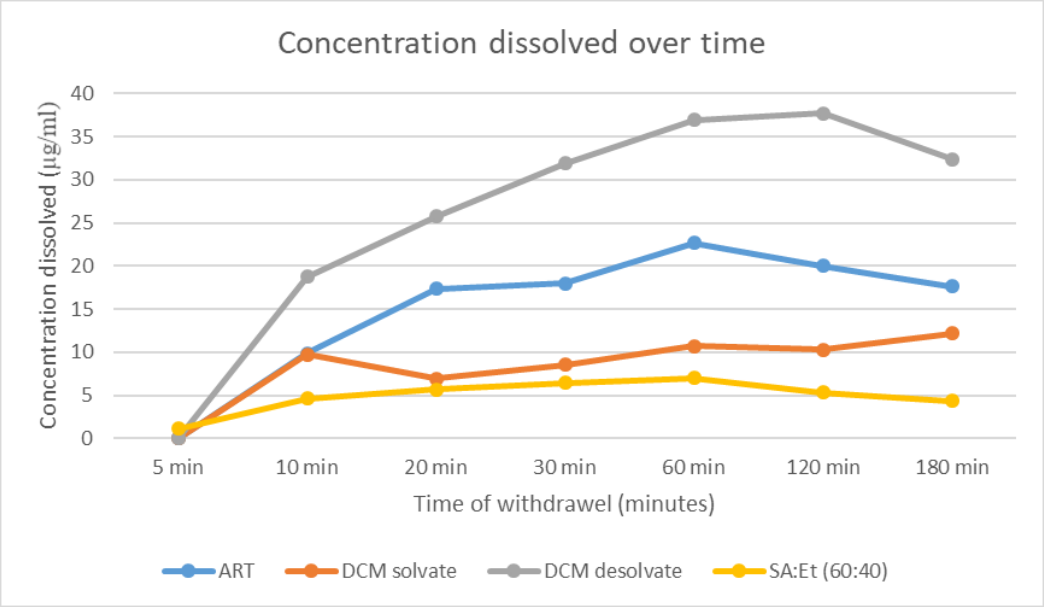

Figure 4.34: Overlay of the four powder dissolution profiles tested.

The powder dissolution experiments were only performed on the representative crystals of every possibly different solid-state form, i.e. Form I (raw material), DCM solvate and DCM desolvate, and the form obtained from the ethanol group. Interestingly although the DCM desolvate also represented polymorphic Form 1, the dissolution results showed a significantly higher concentration (38 µg/ml),

compared to the raw material (23 µg /ml) (Form 1). The DCM desolvate exhibited the best dissolution results. It seemed that the concentration of dissolved ART depended more on the habit, than on the polymorphic form. The SEM photos of the different ART samples tested were unfortunately not that conclusive regarding the differences in habits.

A study by Bezuidenhout (2016) revealed that the ART raw material concentration in water had decreased to 70%, after 3 h of testing (i.e. 30% degradation). Those findings were recorded following a hydrolysis experiment, which, although it differed from the dissolution testing, may have explained the variable and lower dissolution results after 3 h of the ART raw material and each of the recrystallisation products tested.

4.3.6 Thermal microscopy

The different techniques used to obtain the different microscopic images, were performed in accordance with the method, as described in Chapter 3 (par. 3.3.3).

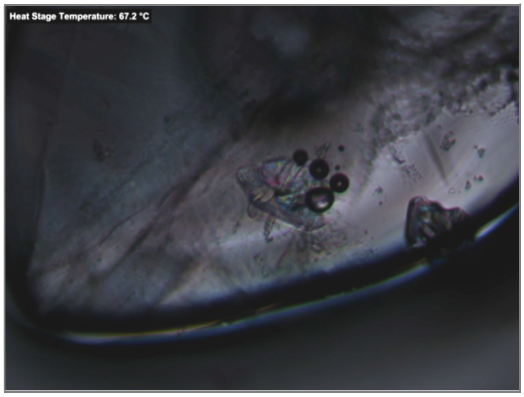

Figure 4.35: Thermal microscopic image of the DCM solvate at 67.2°C, showing the evolution of bubbles.

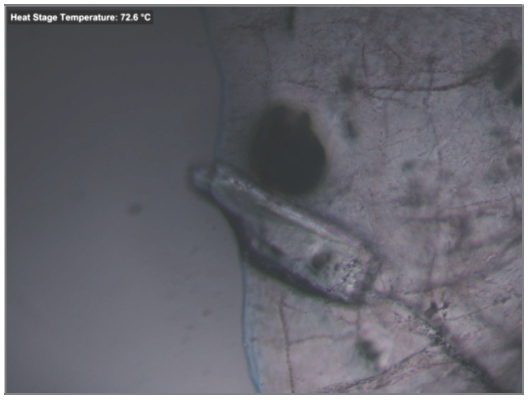

Figure 4.36: Thermal microscopic image of the crystals recrystallised from ACN at 72.6°C.

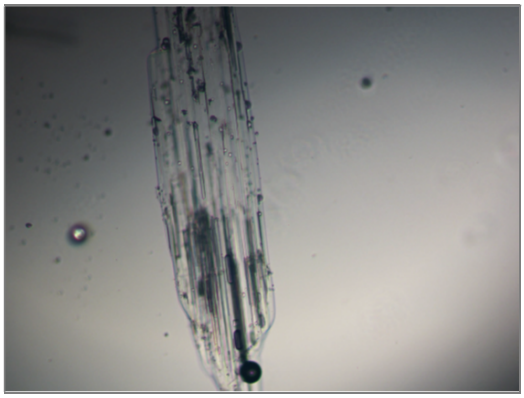

Figure 4.37: Thermal microscopic image of the crystals recrystallised from methanol at 88°C.

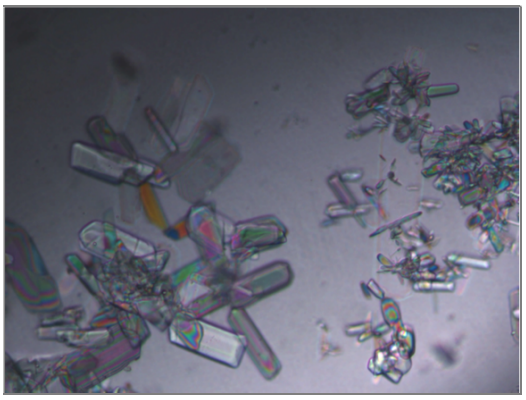

Figure 4.38: Thermal microscopic image of the crystals recrystallised from ethanol at 72°C.

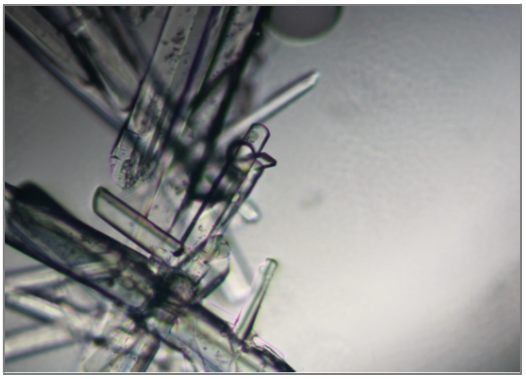

Figure 4.39: Thermal microscopic image of the crystals recrystallised from 1-propanol at 70°C.

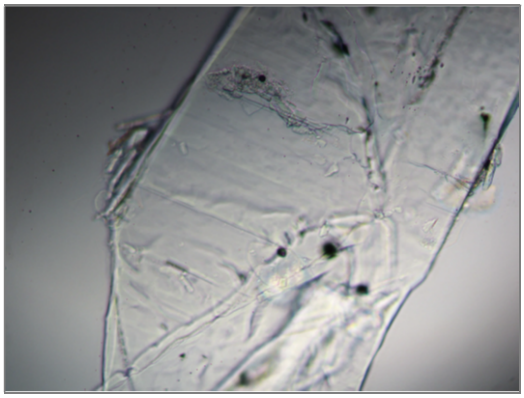

Figure 4.40: Thermal microscopic image of the crystals recrystallised from 2-propanol at 75°C.

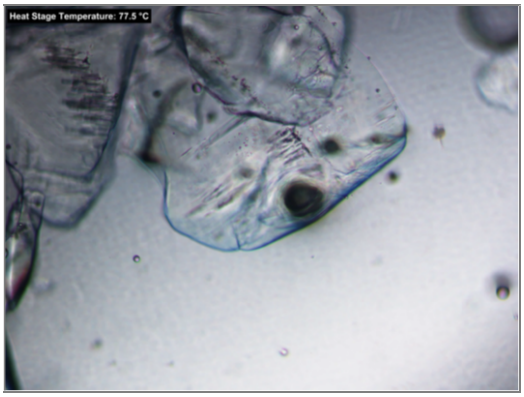

Figure 4.41: Thermal microscopic image of the crystals recrystallised from 2-butanol at 77°C.

The thermal microscopic images were recorded to confirm whether any solvate had possibly formed during the recrystallisation study. Only the DCM recrystallisation product showed the evolution of bubbles, which confirmed the solvate state, as previously mentioned. None of the other recrystallisation products showed any gas evolution, and hence no indication of any solvates.

4.3.7 Stereo microscopic images

During the recrystallisation study, it had become clear that different crystal habits had been formed from the different organic solvents. A few of those habits were photographed to illustrate the morphology of the resulting crystals. The different techniques used to obtain the images were carried out in accordance with the method described in Chapter 3 (par. 3.3.3.2).

The literature uses individual, descriptive, crystal habit terms, like acicular, bladed and blocky, for example (Anon, 2019). Table 4.9 summarises some of the most common terms used for the different crystal habits (Stieger, 2012).

Table 4.9: Summary of the most common crystal habits (Stieger *et al*., 2009)

Descriptive crystal habit	Description	Simplified illustration
Acicular	Needle-like, slender and/or tapered. Thinner than prismatic, but thicker than fibrous.	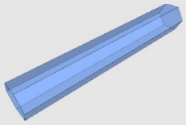
Bladed	Blade-like, slender and flattened. More elongated than platy and thinner than tabular.	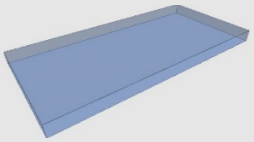
Blocky	Rectangular and box-like, but not necessarily with flat sides. More elongated than equant, less elongated than prismatic and thicker than tabular.	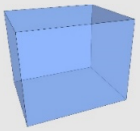
Equant	Any three perpendicular axis through the crystal are more or less equal. Can be used to describe rounded as well as angular crystals.	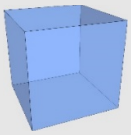
Fibrous	Extremely thin prisms. Thinner than acicular crystals. Occur in either individual crystals or in a tight compact, almost cloth-like mass.	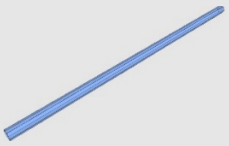
Platy	Flattened and thin crystals (like plates). Wider than bladed and thinner than tabular.	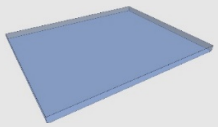
Prismatic	Pencil-like, elongated crystals. Thicker than acicular.	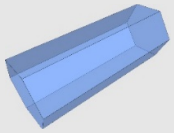
Stubby	Slightly more elongated than equant, but not as elongated as prismatic and possibly more rounded than blocky.	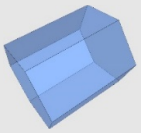
Tabular	Book-like tablets that are thicker than platy, but not as elongated as bladed.	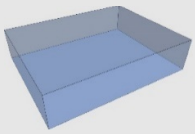

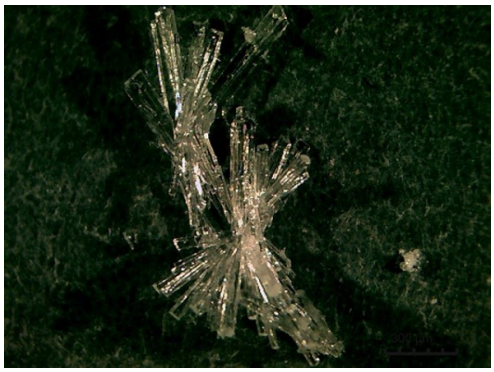	Blade-like, slender and flattened. More elongated than platy and thinner than tabular.	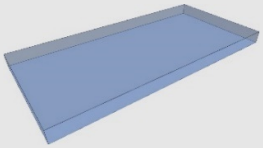

Figure 4.42: Light microscopic image of the recrystallisation product from ethanol at room temperature. According to Table 4.9 it could be described as bladed.

	Pencil-like, elongated crystals. Thicker than acicular.	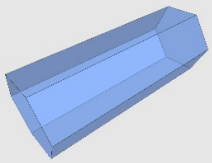

Figure 4.43: Light microscopic image of the recrystallisation product from 2-butanol at room temperature. According to Table 4.9 it could be described as prismatic.

	Slightly more elongated than equant, but not as elongated as prismatic and possibly more rounded than blocky.	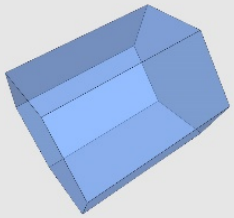

Figure 4.44: Light microscopic image of the recrystallisation product obtained from diethyl ether at room temperature. According to Table 4.9 it could be described as stubby.

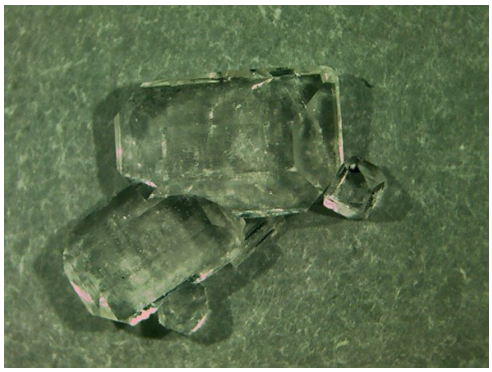	Slightly more elongated than equant, but not as elongated as prismatic and possibly more rounded than blocky.	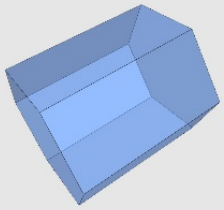

Figure 4.45: Light microscopic image of the recrystallisation product obtained from ethyl acetate at room temperature. According to Table 4.9 it could be described as stubby.

	Rectangular and box-like, but not necessarily with flat sides. More elongated than equant, less elongated than prismatic and thicker than tabular.	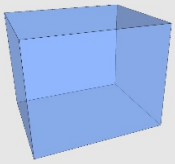

Figure 4.46: Light microscopic image of the recrystallisation product obtained from tetrahydrofuran at room temperature. According to Table 4.9 it could be described as blocky.

Some of the recrystallisation products showed different habits. Although those habits did differ markedly, it was not always indicative of a new solid-state form.

4.3.8 Scanning electron microscopy (SEM)

During the recrystallisation study, it had become clear that different crystal habits had been formed from the different organic solvents. A few of those habits were photographed to illustrate the morphology of the crystals. The different techniques used to obtain the different photos were done according to the method as described in Chapter 3 (par. 3.3.3.3).

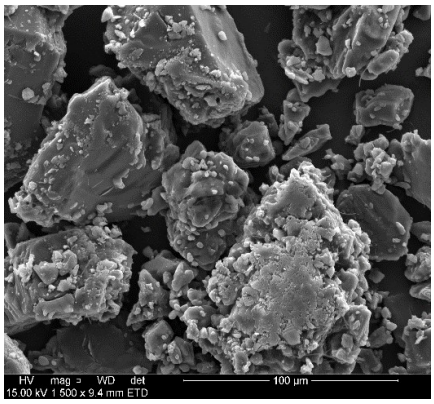	ART raw material
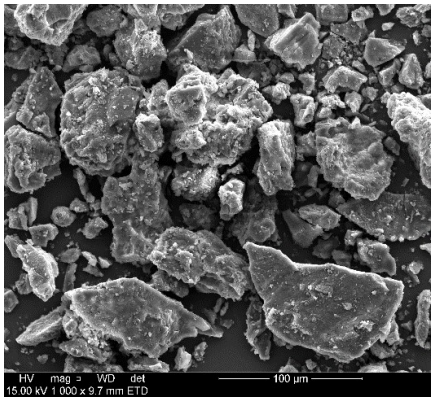	ART DCM desolvate
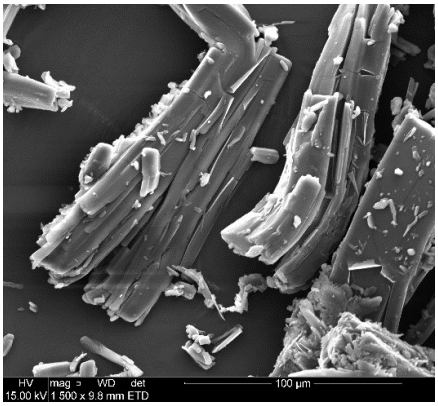	ART ethanol:water mixture (60:40).

Figure 4.47: SEM micrographs of ART samples.

The DCM desolvate appeared more brittle than the ART raw material, whereas the ethanol:water (60:40) mixture was presented as blade-like crystals.

4.4 Conclusion

A novel solvate of artesunate raw material was described in this chapter, i.e. DCM solvate. A few possible new polymorphic forms were identified during this study, which will require confirmation by further studies, as well as through single X-ray crystallography determinations. Contradictory results had been obtained for the recrystallisation product obtained from acetone. The XRPD analysis showed that the crystals were similar to that of Form I, while the FT-IR spectrum differed significantly from Form I. The possibility of desolvation having occurred during sample preparation was mentioned, since the XRPD sample preparation had involved grinding of the crystals, whereby desolvation could have occurred.

The different recrystallisation products showed different habits, as demonstrated by the scanning electron microscopy and the stereo microscopy photos. The powder dissolution results of ART were low due to the poor solubility of ART in water. The DCM desolvate, however, surprisingly showed the best powder dissolution results. Although the DCM desolvate also represented Form 1, this drastic increase in dissolution results could possibly have been the result of the differences in habit between the different crystal forms of ART. Unfortunately, the SEM photos did not clarify this phenomenon, but a larger particle surface area could have played a role in the better dissolution results.

Further investigations should be performed to clarify the possibility of the new polymorphic forms, and also to investigate the dissolution results obtained with the dichloromethane desolvate.

References

Anon. 2019. What are descriptive crystal habits? http://www.galleries.com/minerals/property/habits.htm [Date of access: 29 July 2019].

Bezuidenhout, J. W. 2016. Solid-state characterisation of artesunate. Potchefstroom:NWU. (M.Sc. Dissertation). 102p.

Byrn, S.R., Pfeiffer, R.R. & Stowell, J.G. 1999. Solid-state chemistry of drugs. SSCI Inc: West Lafayette. p222-259.

Caira, M.R. 2019. Artesunate polymorphic forms. Technical report.

Lisgarten, J.N., Potter, B., Palmer, R.A., Chimanuka, B. & Aymami, J. 2002. Structure, absolute configuration, and conformation of the antimalarial drug artesunate. *Journal of Chemical Crystallography*, 32: 43-48.

Stieger, N. 2009. Polymorphism and physico-chemical properties of nevirapine. Potchefstroom:NWU. (Thesis-PhD). 154p.

Chapter 5

Summary and conclusion

In Chapter 1, an overview of the different solid-state forms in which active pharmaceutical ingredients (APIs) can exist, was given. Every solid-state form has unique physico-chemical properties, which may influence its stability and manufacturing capabilities. A change in the solid-state form of an API, especially during manufacturing, may render unexpected stability and/or manufacturing problems, for example.

Various definitions for polymorphism were also discussed in Chapter 1, of which the definition by Haleblian and McCrone (1969) is the most popular and best descriptive, as it states that: 'A polymorph is a solid crystalline phase of a given compound resulting from the possibility of at least two different arrangements of the molecule of the compound in the solid-state. Polymorphism is thus the ability of any molecule or compound to crystallise as more than one distinct crystal species.'

The physico-chemical properties of artesunate (ART) and its structure, solid-state forms and pharmacology, were discussed in Chapter 2. ART is a derivative from artemisinin and has been used effectively as treatment against malaria, since 2003 (Li & Weina, 2010). Malaria poses a major health risk to humans and since drug resistance had become a major issue, new alternatives have been explored and were the artemisinin derivatives introduced. According to the World Health Organization (WHO, 2015), the artemisinin-based combination therapies are currently the preferred choice for the treatment of uncomplicated *Plasmodium falciparum* (*P. falciparum*) malaria.

Regarding the solid-state forms of ART, a Form 1 polymorphic form is described in the literature, which is currently the commercially available form of the ART raw material. No other polymorphic forms of ART, nor solvates, nor hydrates, are described in the literature to date.

Since ART is classified as a Class II drug, according to the Biopharmaceutical classification system (BCS) (low solubility and low permeability), it made sense to explore other possible solid-state forms of ART in an effort to improve its solubility. This study further aimed at investigating whether ART would produce other polymorphic forms than the one already reported in the literature.

Chapter 3 outlined all of the preparation and characterisation methods used to identify any possible new ART solid-state forms. The characterisation methods were discussed and the data collected through those techniques in order to characterise each ART recrystallisation product. The typical solid-state characterisation methods used were X-ray powder diffractometry (XRPD), Fourier-transform infrared spectroscopy (FT-IR), thermal analysis, microscopy and dissolution studies. Where needed, and where good quality single crystals were formed, single X-ray crystallography was performed.

In Chapter 4, all the results from the characterisation methods carried out on the different recrystallisation products, were discussed. Various super-saturated solutions of ART had been prepared, by using different organic solvents, and the solvents allowed to evaporate at room temperature. According to the different solid-state characterisation techniques employed during this study, the crystals that had been obtained through slow recrystallisation from various solvents, could be classified into the following three groups:

Form 1: ART raw material, and crystals obtained from diethyl ether, ethyl acetate, tetrahydrofuran, 1-butanol, 2-butanol and the dichloromethane (DCM) desolvate.

A novel solvate: DCM solvate (confirmed with single X-ray crystallography).

New possible polymorphic forms: Crystals obtained from the recrystallisation from acetonitrile (ACN), acetone methanol, ethanol, from different ethanol:water mixtures, 1-propanol, 2-propanol and from methanol:water (50:50). All these new forms obtained, would need to be further investigated and where possible, single X-ray crystallography would be required to confirm their statuses.

The powder dissolution experiments were only performed on the ART raw material (Form I), DCM solvate, DCM desolvate and on the possibly new form obtained through recrystallisation from the ethanol group. Interestingly, although the DCM desolvate also represented polymorphic Form 1, its dissolution results showed a significantly higher dissolution concentration (38 µg/ml), compared to the ART raw material (23 µg /ml) (Form 1). The DCM desolvate had exhibited the best dissolution results. It seemed that the concentration of dissolved ART had probably depended more on the crystal habit, than the polymorphic form. The scanning electron microscopy (SEM) photos of the different ART samples tested, were unfortunately not definitely conclusive regarding the differences in habits of the recrystallisation products.

Further investigations should be performed to clarify the possibility that any new polymorphic forms of ART had been prepared during this study, and also to investigate the dissolution results obtained with the DCM desolvate sample.

References

Haleblian, J. & McCrone, W. 1969. Pharmaceutical applications of polymorphism. *Journal of Pharmaceutical Sciences*, 58(8): 911-929.

Li, Q. & Wiena, P. 2010. Artesunate: the best drug in the treatment of severe and complicated malaria. Pharmaceuticals, 3(7):2322-2332.

WHO *see* World Health Organization.

World Health Organization (WHO). 2015. Guidelines for the treatment of malaria. World Health Organization. https://www.who.int/malaria/publications/atoz/9789241549127/en/ [Date of access: April, 2019].

Annexures

Annexure A: Complete XRPD determination data

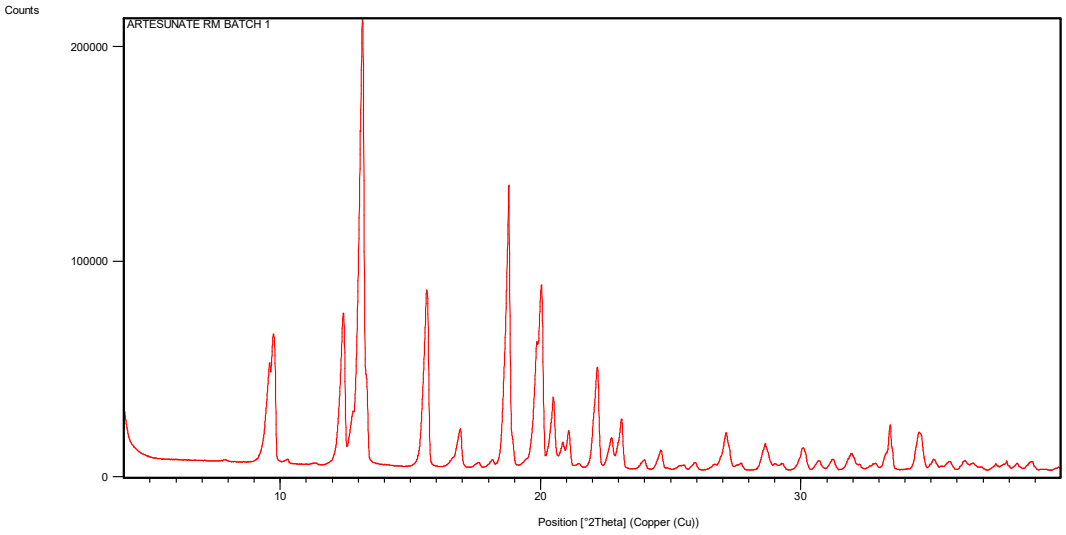

Figure A.1 XRPD pattern of ART raw material (Form I).

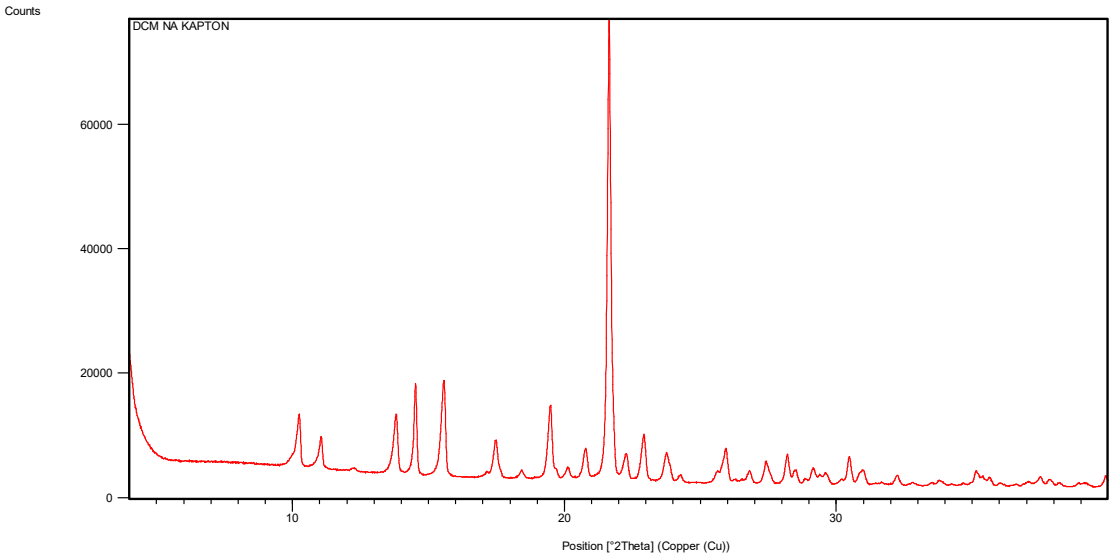

Figure A.2 XRPD pattern of dichloromethane solvate

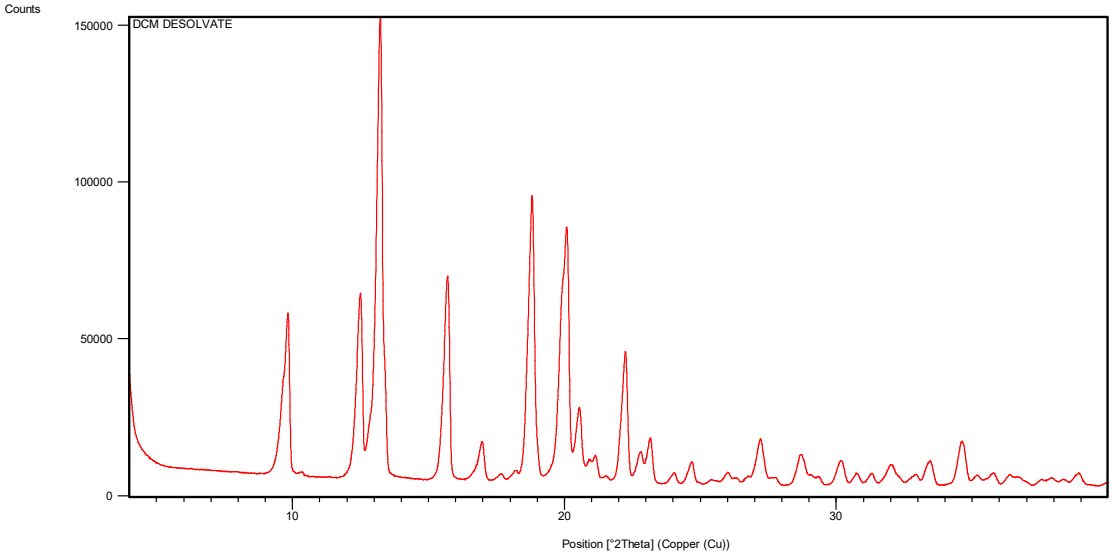

Figure A.3 XRPD pattern of dichloromethane desolvated crystals.

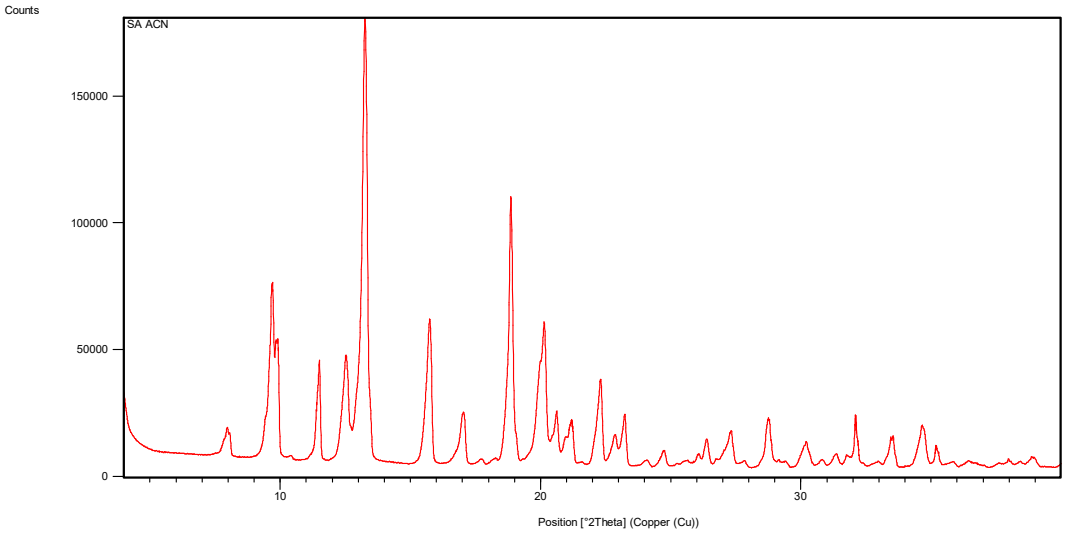

Figure A.4 XRPD pattern of crystals obtained from acetonitrile

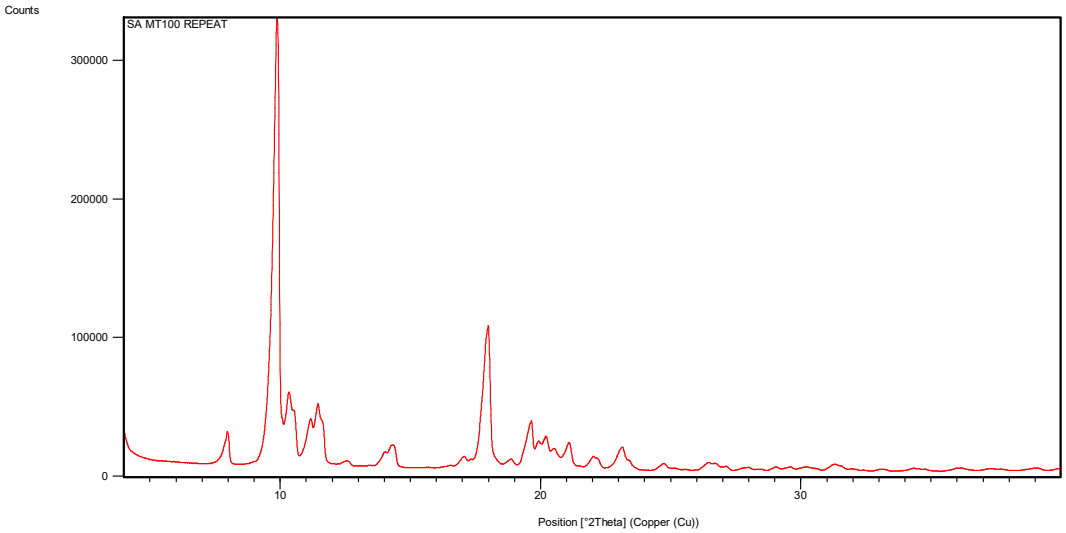

Figure A.5 XRPD pattern of crystals obtained from methanol

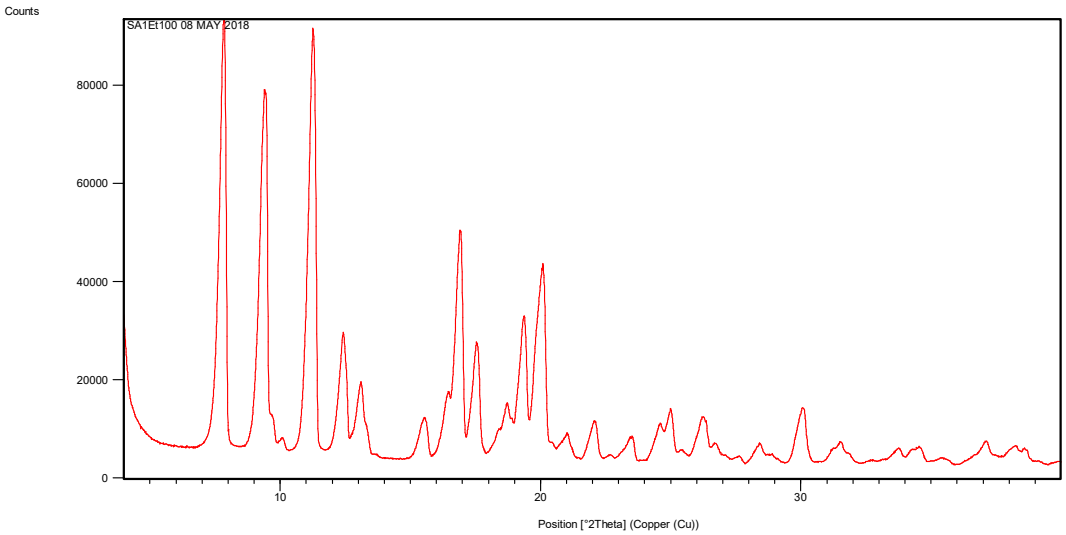

Figure A.6 XRPD pattern of crystals obtained from ethanol

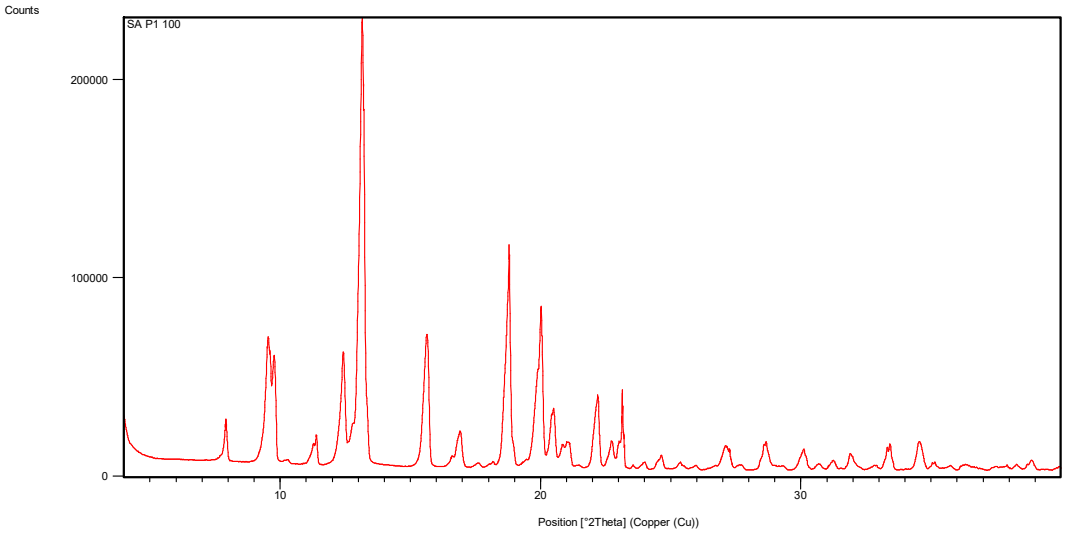

Figure A.7 XRPD pattern of n-propanol

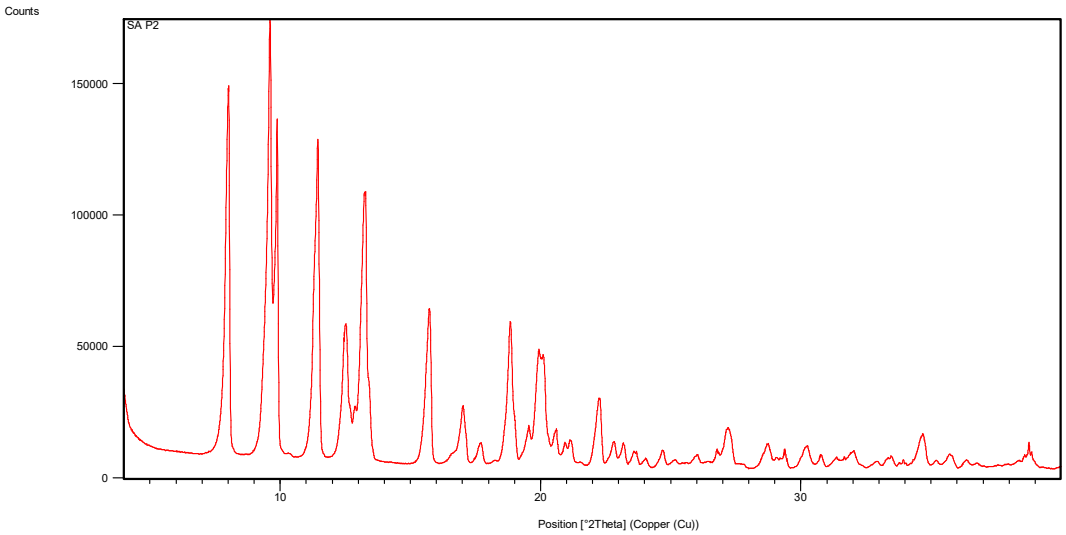

Figure A.8 XRPD pattern of 2-propanol

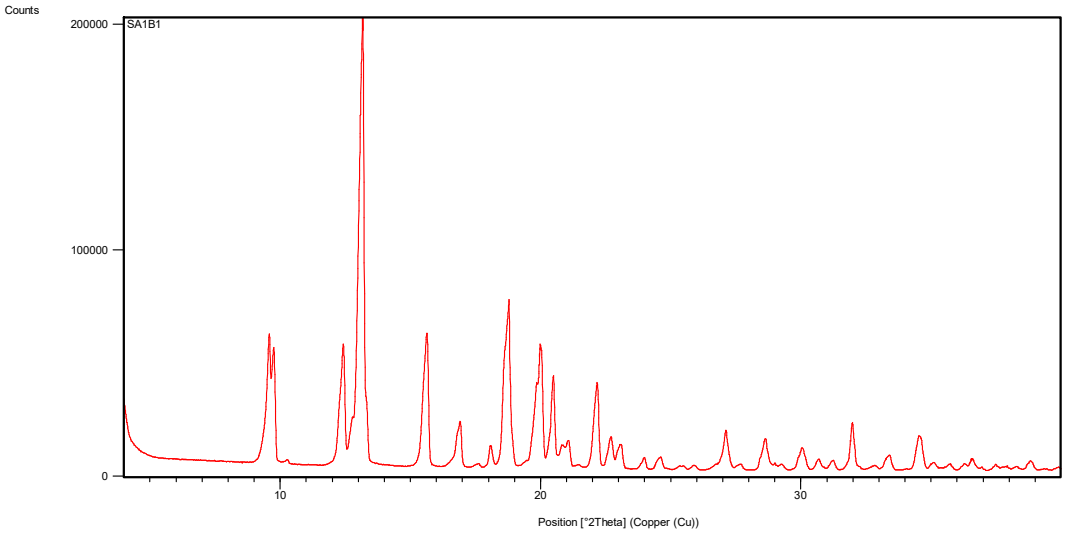

Figure A.9 XRPD pattern of n-butanol

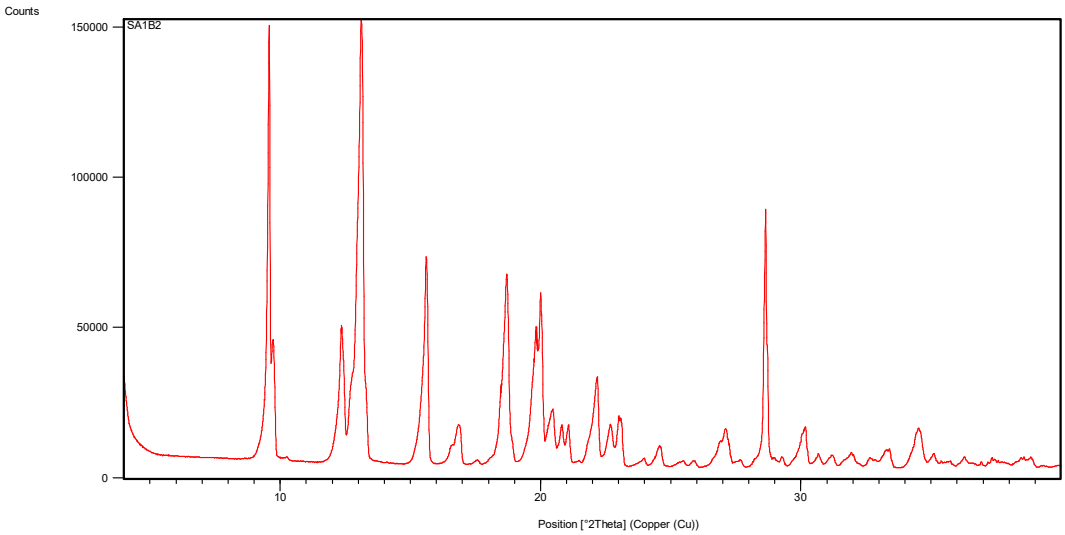

Figure A.10 XRPD pattern of 2-butanol

Annexure B:

BRIEF REPORT: X-RAY STRUCTURE OF THE ARTESUNATE DCM SOLVATE

Experimental

Several crystals were tested for their diffraction quality to optimise the data-collection quality. Eventually a single crystal of dimensions given in Table 1 (p.2) was cut from a larger crystal under mother liquor to avoid solvent loss. X-ray data-collection (48 h) was carried out on a Bruker Apex II Duo diffractometer with the crystal under a nitrogen cold-stream maintained at 100(2) K.

Following data-reduction and correction for absorption effects, space group determination was not routinely determined by the software employed (program X-Prep) and therefore a manual determination was performed by identifying the diffraction symmetry and systematic absences. This led to the conclusion that the crystal system was trigonal and that the space group was either $P3_1$ or its enantiomorphous alternative $P3_2$. The correct choice was critical as this would determine the absolute configurations at all chiral centres of the artesunate molecule. The space group $P3_1$ was selected arbitrarily and the structure was solved by direct methods and refined by full-matrix least-squares methods.

The asymmetric unit revealed in the Fourier electron-density map comprised two crystallographically independent molecules of artesunate and three independent molecules of dichloromethane (DCM). Isotropic refinement of all non-hydrogen atoms yielded acceptable thermal vibration parameters and anisotropic refinement followed. Abnormally high thermal vibration of the chlorine atoms of one of the DCM molecules was evident. An attempt to model this abnormal motion using the technique of including 'split' atoms with appropriate C-Cl distance constraints was not successful due to model instability and the final refinement involved standard anisotropic treatment as a realistic alternative. Finally, it was possible to locate all H atoms in successive difference Fourier maps (an indication of high-quality diffraction data) and they were included in the model in idealised positions based on those determined experimentally and with isotropic thermal parameters related to those of their parent atoms.

The value of the Flack parameter (Table 1) was very close to zero with a small standard deviation, leaving no doubt that the space group $P3_1$ was the correct choice. A subsequent check of the structural models of the two independent artesunate molecules in the asymmetric unit showed that their chiral centres had absolute configurations consistent with those corresponding to 10-α-artesunate.

The structure of the asymmetric unit is shown in Figure 1 (p.3).

Table 1 - Crystal Data and Details of the Structure Determination

Crystal Data	
Formula	$2(C_{19}H_{28}O_8)$, $3(CH_2Cl_2)$
Formula Weight	1023.60
Crystal System	Trigonal
Space group	$P3_1$ (No.144)
a, b, c [Å	10.5907(12) 10.5907(12) 37.045(4)
alpha, beta, gamma [°]	90 90 120
V [$Å^3$]	3598.4(10)
Z	3
D(calc) [g/cm^3]	1.417
μ(MoKa) [/mm]	0.425
F(000)	1614
Crystal Size [mm]	0.20 x 0.23 x 0.31
Data-Collection	
Temperature (K)	100(2)
Radiation [Å]	MoKa 0.71073
Theta Min-Max [°]	1.6, 28.4
Dataset	-14: 14; -14: 14; -49: 49
Tot., Uniq. Data, R(int)	109367, 11947, 0.090
Observed data [I > 2.0 sigma(I)]	10969
Refinement	
Nref, Npar	11947, 576
R, wR_2, S	0.0467, 0.1103, 1.04
$w = 1 / [\sigma^2(F_o^2) + (0.0421 P)^2 + 3.46 P]$ where $P = (Max (F_o^2, 0) + 2 F_c^2) / 3$	
Max. and Av. Shift/Error	0.00, 0.00
Flack x	-0.05(2)
Min. and Max. Resd. Dens. [e $Å^{-3}$]	-1.01, 1.03

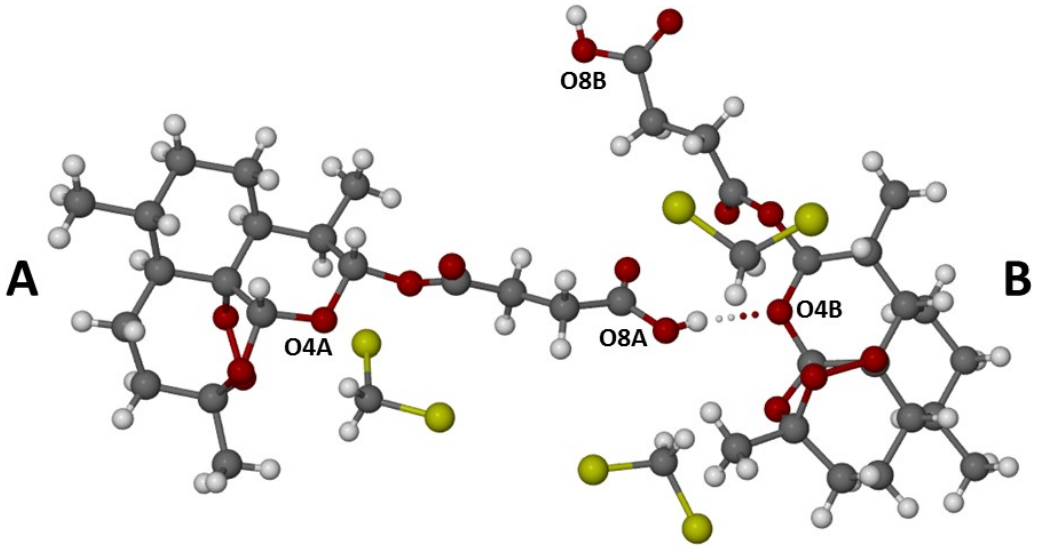

Figure 1. The asymmetric unit of the solvate, consisting of two independent molecules of artesunate and three independent dichloromethane molecules.

In Figure 1, atoms that are involved in classical hydrogen bonding are labelled. One of the two unique O-H···O hydrogen bonds is shown, namely that between the -COOH group of artesunate molecule A and the pyranose oxygen atom O4B of artesunate molecule B. Geometrical details are: H-bond designation O8A-H8A···O4B, with O8A···O4B 2.805(5) Å and angle O8A-H8A···O4B 164°.

In the crystal, the independent artesunate molecules are linked to one another *via* head-to-tail hydrogen bonding as shown in Figure 2. This results in the roughly planar zigzag ribbon-motif with infinite rows of A molecules on the left and B molecules on the right, propagating parallel to the crystal *b*-axis.

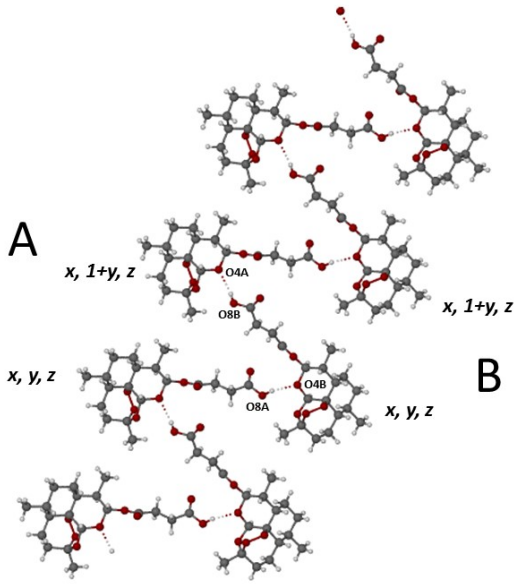

Figure 2. Zigzag ribbon-r nd B molecules.

The second of the two unique O-H···O hydrogen bonds, O8B-H8B···O4A^{i} (i = *x, 1+y, z*), is shown in Figure 2. This H-bond is geometrically similar to that shown in Figure 1. In this case, the details are as follows: O8B ···O4A^{i} = 2.806(4) Å, O8B-H8B···O4A^{i} angle 153°.

In addition to the intermolecular O-H···O hydrogen bonds that link the artesunate molecules, the crystal structure is stabilised by numerous C-H···O hydrogen bonds which also link artesunate molecules. For clarity at this stage, the latter are not shown in Figure 3, but C-H···O hydrogen bonds involving the acidic H atoms in the DCM molecules as donors are shown bound to artesunate oxygen atoms, indicating the role of the solvent molecules which reside between the zizag artesunate ribbons. There is also one instance of a C-H···Cl H-bond, the C-H group being that of a DCM molecule.

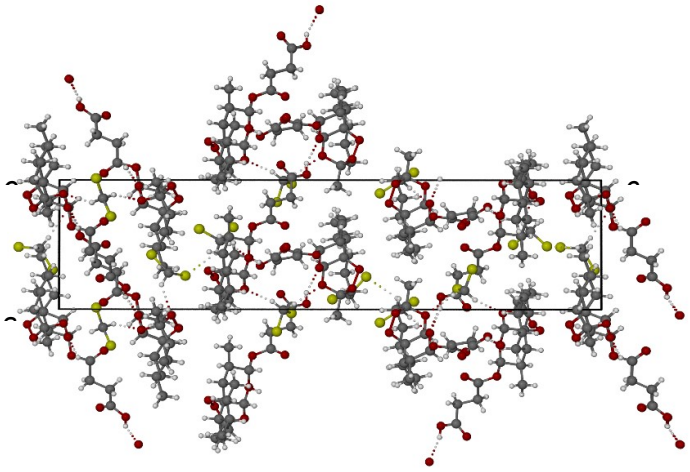

Figure 3. Crystal packing diagram showing O-H···O hydrogen bonds linking the artesunate molecules and C-H···O and C-H···Cl hydrogen bonds that involve DCM C-H donor groups.

The simulated PXRD pattern for the solvate computed from the fully refined crystal structure is shown below (Figure 4) together with the experimental PXRD pattern obtained from Potchefstroom. (This is a crude comparative diagram that can later be improved and re-formatted when necessary).

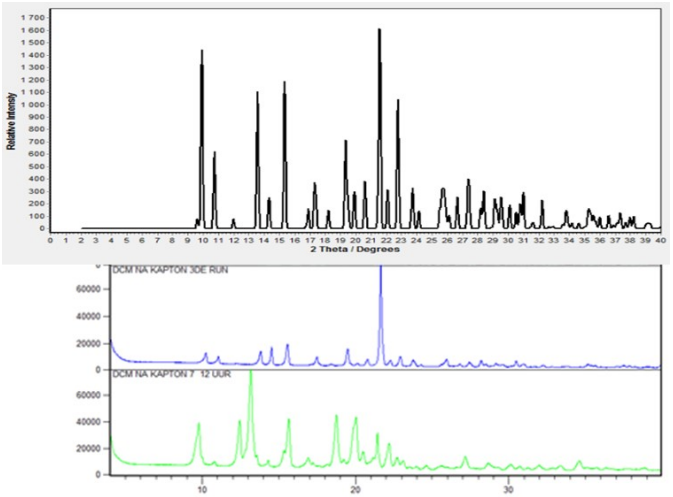

Figure 4. PXRD pattern of the DCM solvate computed from the single crystal structure (top) and the experimental trace (blue).

Differences in peak position can be attributed to the temperature differences (simulated, 100 K; experimental 'room temperature' assumed). There is a fairly reasonable peak correspondence, but this could very likely be improved significantly by reducing the preferred orientation that is evident in the sample.